Vol. 10
Issue 2
Fall 2021

# ASSAYWISE LETTER

LIFE SCIENCE RESOURCES AND APPLICATIONS

## Uncover the Full Spectrum of Possibilities

### Featuring

Fluorescent Probe Technologies Suitable for Multicolor Spectral Flow Cytometry

Portelite™ Fluorimetric Quantitation Kits: Companion Reagents Optimized for the CytoCite™ BG100 Spectrofluorometer

Frontiers in Serodiagnostics: A New Plasmon-Enhanced Fluorescence Biosensor Technology Suitable for Lab-on-a-Chip Applications

Fluorescent Tools for Studying Mitochondrial Morphology and Function

AAT Bioquest®

# Table of Contents

# Portelite™ Fluorimetric Quantitation Kits

## Companion Reagents Optimized for the CytoCite™ BG100 Spectrofluorometer


### *Abstract*

*Portelite™ Fluorimetric Quantitation Kits, optimized for AAT Bioquest's CytoCite™ BG100 fluorometer, are designed to selectively quantify total nucleic acid, DNA (ssDNA, dsDNA), RNA, endotoxin, and protein, providing more sensitive analysis than comparable UV absorbance-based instrumentation. The aforementioned kits are suitable for a variety of common biological applications, including cloning, sequencing, transfection, qPCR, lipopolysaccharide (LPS) detection, and gel electrophoresis. All assays are performed using the same general protocol, providing a simple mix-and-read assay format. Kits contain concentrated assay reagent, dilution buffer, and pre-diluted standards. The fluorescent probes in each kit have similar spectral properties, being blue light-excitable (480 nm), with emissions between 510 nm and 580 nm. While developed specifically for use with the CytoCite™ BG100 fluorometer, Portelite™ Fluorometric kits may also be used on other commercially available compact fluorometric instruments, such as the Qubit® fluorometer (Thermo Fisher, Inc.).*


## Introduction

Conventional cuvette-based spectrophotometers consume relatively large amounts of precious biological samples. Consequently, compact instruments were devised to address the need to employ biomolecular assays using progressively smaller amounts of sample. For example, the NanoDrop microvolume spectrophotometer (Thermo Scientific) combines fiber optic technology and sample surface tension properties to capture and retain small amounts of material without needing cuvettes or capillaries (Desjardins and Conklin, 2010).

A similar requirement for high-sensitivity fluorescence-based assays, using limited amounts of sample, has led to the development of several compact spectrofluorometers. Unlike the Nanodrop line of compact spectrophotometers which quantify absorbance, measurements performed by the CytoCite™ (AAT Bioquest) and Qubit® (Thermo Scientific) compact fluorometers rely upon the principle of fluorometry, wherein quantification of as little as 1 mL of DNA, RNA, or protein sample is achieved with high accuracy by employing sensitive fluorescent dyes. Compared with absorbance-based measurements, fluorescence-based measurements exploiting dye-binding are more precise, selective, and sensitive for quantifying different classes of biomolecules (Table 1; Khetan et al., 2019). For instance, optimized intercalating fluorescent dyes have been developed to interact specifically with double-stranded DNA (dsDNA), and thus their quantification is not impacted significantly by contaminating proteins, single-stranded DNA (ssDNA), or RNA molecules.

Absorbance-based methods, as employed by the Nanodrop spectrophotometer, cannot selectively monitor dsDNA, ssDNA, RNA, and nucleotides, as only total sample absorbance is measured. Additionally, with spectrophotometry, nucleic acids are typically measured using their absorbance maxima of 260 nm, while proteins are measured using their absorbance maxima

of 280 nm. The ratio of 260 nm-to-280 nm is often employed to monitor sample purity obtained after DNA and RNA extraction (Manchester, 1996). However, inaccurate ratios are often encountered, especially at very low sample concentrations (<10 ng/µL) of nucleic acids, contributing to inaccurate concentration estimates provided by the NanoDrop instrument. This is particularly true, for instance, when monitoring circulating free DNA fragments (cfDNA) released into the blood plasma (Ponti, 2018; Khetan et al., 2019). With fluorometers, such as the Qubit® and CytoCite™ instruments, deploying fluorescent dyes that are relatively selective for dsDNA, ssDNA, total nucleic acid, RNA, and protein minimizes the impact of any contaminants in the sample that would otherwise produce spurious results during quantification. Successful application of fluorescence-based sample quantification depends upon optimal pairing of a suitable analytical instrument with high-performance reagents.

## CytoCite™ BG100 Portable Fluorometer

The CytoCite™ BG100 instrument is a cloud-integrated, palm-sized fluorometer optimized to detect probes in the ubiquitously employed FITC channel (Ex/Em = 480 nm/520 nm), with an overall limit of detection of as little as 1 nM of fluorescein (Figure 1). For red fluorescence-emitting probes (Ex/Em = 530 nm/620 nm), such as resorufin-based Amplex™ Red and Amplite® Red peroxidase substrate assays, the CytoCite™ GR100 instrument is recommended. With a small footprint, the CytoCite™ BG100 and CytoCite™ GR 100 portable fluorometers are the most compact fluorometers available on the market, facilitating easy integration into any laboratory, point-of-care use, or field testing environment. As the only commercially available cloud-enabled fluorometer, the CytoCite™ Fluorometer offers several significant advantages relative to other instruments, such as the Qubit® Fluorometer (Thermo Fisher). Primary differentiating features include:

1. Unlimited storage of sample results
2. Automated daily data backups to prevent unexpected data loss
3. Synchronization of sample results across different analysis platforms, accessible from any authenticated device, such as a smartphone
4. Compatibility with AAT Bioquest's comprehensive Quest Graph™ analytical suite of tools for fast and easy regression modeling, $IC_{50}$ calculations, and more

The CytoCite™ Fluorometer utilizes sample volumes of as little as 1 uL and is several orders of magnitude more sensitive than absorbance-based instruments, such as the Nanodrop™ (ThermoFisher) for both DNA (absorbance = 260 nm) and protein

**Table 1.** Comparison of representative compact fluorescence- and absorbance-based spectrometers.

| Attribute | CytoCite™ BG100 Spectrofluorometer | UV-absorbance-based, microliter volume spectrophotometer |
|---|---|---|
| **Quantification Approach** | Fluorescent dyes bind specifically to ssDNA, dsDNA, total nucleic acid, RNA, protein or endotoxin.<br>High selectivity. | UV absorbance measurements (absorbance at 260 nm and 260 nm/280 nm ratio).<br>Poorer selectivity. |
| **Selectivity for ssDNA vs dsDNA** | Accurately measures both dsDNA and ssDNA from the same sample. | Results for samples containing both are inconclusive—cannot distinguish one from the other. |
| **Selectivity for DNA vs RNA** | Accurately measure both DNA and RNA from the same sample. | Results for samples containing both are inconclusive—cannot distinguish one from the other. |
| **Accuracy/Precision for Low Concentrations** | Typically, sub ng/µL detection of dsDNA | Fails to accurately quantify NGS samples containing <40 ng/µL DNA. Fails to accurately quantify cfDNA containing ~50 ng/µL. |
| **Dynamic Range** | Fluorescence-based assay with 4-5 orders of magnitude linear dynamic range. (10 pg/µL to 1 µg/µL DNA) | Absorbance based assay. Linear dynamic range limited to 2-3 orders of magnitude. (2 ng/µL to 15 µg/µL) |
| **Detection of Endotoxin Contamination** | Fluorescence-based assay with 4-5 orders of magnitude linear dynamic range. (10 pg/µL to 1 µg/µL DNA) | Poorer sensitivity due to chromogenic substrate. |
| **Cost** | $$ | $$$$ |

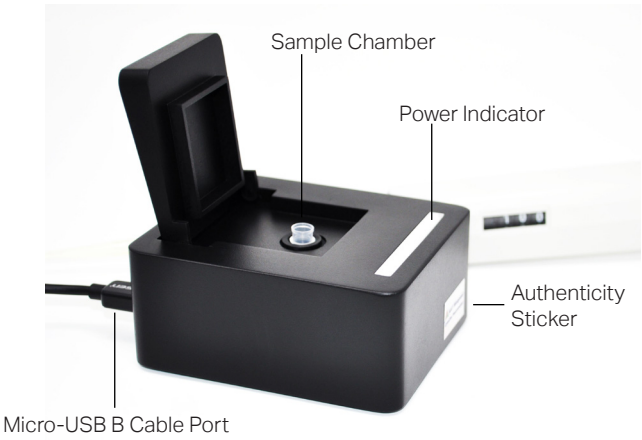


**Figure 1.** The CytoCite™ BG100 Spectrofluorometer.

## CytoCite™ Instrument Specifications

| | |
|---|---|
| **Dimensions** | 3.54"L x 2.83"W x 1.54"H (9.0 cm x 7.2 cm x 3.9 cm) |
| **Weight** | ~0.3 lbs (135 g) |
| **Operating Ranges** | 10 - 30 °C; < 80% relative humidity |
| **Installation Location** | Indoor use only |
| **Typical Power Consumption** | 2.5 VA |
| **Power Requirements** | 5 VDC, 0.5 A |
| **Computer Interface** | Micro-USB B, USB 2.0 |
| **Dynamic Range** | 5 orders of magnitude |
| **Light source (device dependent)** | Blue LED (max ~470 nm) (Cat No. CBG100)<br>Green LED (max ~530 nm) (Cat No. CGR100) |
| **Excitation Filter (device dependent)** | Blue 457 - 487 nm (Cat No. CBG100)<br>Green 517 - 547 nm (Cat No. CGR100) |
| **Emission Filter (device dependent)** | Green 515 - 565 nm (Cat No. CBG100)<br>Red 610 - 665 (Cat No. CGR100) |
| **Detector** | Photodiode |
| **Tube Type** | 0.2 mL clear, thin-wall PCR tubes |
| **Minimum Assay Volume** | 150 µL |

(absorbance = 280 nm) quantification. It is also compatible with a comprehensive library of bioassays and fluorometric reagents, allowing for rapid, repeatable quantification of small molecules such as calcium, mercury, RNA, DNA, protein, and endotoxin.

## Key Applications for Portelite™ Fluorometric Quantitation Kits

### Total Nucleic Acid Detection

The Portelite™ Fluorimetric Total Nucleic Acid Quantitation Kit (17631) measures the total quantity of nucleic acids, including dsDNA, ssDNA, and RNA, in an easy and accurate format. The kit provides all the essential reagents, including Helixyte™ Green All reagent, dilution buffer, and pre-diluted DNA standards. The Helixyte™ Green All reagent (Ex/Em = 509/529 nm) is a sensitive fluorescent nucleic acid probe for measuring the total quantity of nucleic acids in a sample that may contain dsDNA, ssDNA, RNA, and long oligonucleotides. Helixyte™ Green All reagent indiscriminately binds to dsDNA, ssDNA, and RNA. The kit is optimized for measuring the total amounts of nucleic acids using the CytoCite™ or Qubit® fluorometers.

### DNA Detection

In biomedical research laboratories, DNA quantification represents a fundamental procedure required in most molecular biology protocols, including polymerase chain reaction (PCR) amplification and next-generation sequencing (NGS). An assortment of methods is available for DNA quantification, including UV absorbance, agarose gel electrophoresis, and fluorescent DNA-binding dye techniques. The CytoCite™ and Qubit® instruments are particularly useful for monitoring DNA quality prior to NGS because of their ability to measure intact dsDNA. Importantly, unlike absorbance-based devices, these fluorescence-based systems can readily determine the amount of intact dsDNA, and the quantitative value yielded decreases with the level of fragmentation and denaturation of DNA. Fluorescence spectroscopy is better able than absorbance to evaluate the template activity of DNA for PCR. While qPCR might seem the optimal choice in this context, the procedure is much more time-intensive and expensive than fluorometry.

The Portelite™ High Sensitivity DNA Quantitation Kit (17660, 17661) provides a rapid method to quantify dsDNA using Helixyte™ Green fluorescent dye (Ex/Em = 502/522 nm). The assay is linear over five orders of magnitude of concentration and is highly selective for dsDNA relative to ssDNA and RNA. The kit is designed to be accurate for initial sample concentrations ranging from 1.25 pg/mL to 100 ng/mL. Helixyte™ Green dye exhibits significant fluorescence enhancement upon binding to dsDNA and provides sensitivity that is a few orders of magnitude better than UV absorbance-based assays.

The Portelite™ Fluorimetric DNA Quantitation Kit with Broad Dynamic Range (17665) provides a rapid method to quantify dsDNA with Helixyte™ Green BR dye (Ex/Em = 503/527 nm). This Portelite™ Fluorimetric DNA Quantitation assay is linear over three orders of magnitude. The assay is highly selective for double-stranded DNA (dsDNA) relative to RNA and is optimized for measuring dsDNA concentrations ranging from 10 pg/µL to 10 ng/µL. Helixyte™ Green BR dye exhibits large fluorescence enhancement upon binding to dsDNA and provides sensitivity that is a few orders of magnitude better than UV absorbance-based assays. The abovementioned kits differ with respect to the concentration range of dsDNA assayed, but each is optimized for the CytoCite™ and Qubit® fluorometers.

Single-stranded DNA plays an essential role in DNA sequencing. In high-throughput sequencing, the sample dsDNA is processed and fragmented. The resulting ssDNA fragments are attached to a glass slide and then base-paired and amplified with a polymerase. The Portelite™ Fluorimetric ssDNA Quantitation Kit (17625) measures single-stranded DNA in an easy and accurate format (Figure 3). This kit includes the Helixyte™ Green ssDNA reagent (Ex/Em = 498/519 nm), dilution buffer, and pre-diluted DNA standards for ~200 tests. Helixyte™ Green ssDNA reagent is a sensitive fluorescent nucleic acid probe for quantifying oligonucleotides and single-stranded DNA (ssDNA) in solution. It can quantify as little as 100 pg/mL oligonucleotide or ssDNA, a sensitivity exceeding absorbance-based methods by more than 10,000-fold. With this kit, as little as 1 ng/mL oligonucleotide or ssDNA can be detected. The Portelite™ ssDNA Quantitation Kit is optimized for quantifying dsDNA using CytoCite™ and Qubit® fluorometers.

## RNA Detection

Detection and quantification of small amounts of RNA are crucial to a wide variety of biomedical applications, including measuring

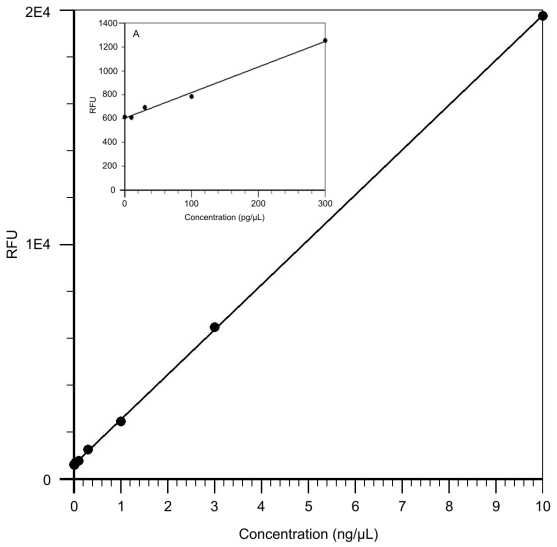


**Figure 2.** The total nucleic acid standard curve was generated using Portelite™ Fluorimetric Total Nucleic Acid Quantitation Kit. 0.15 to 10 ng/µL DNA standard dilutions are shown (> 50-fold linear dynamic range). Inset A shows the lower detection limit can extend down to 10 pg.

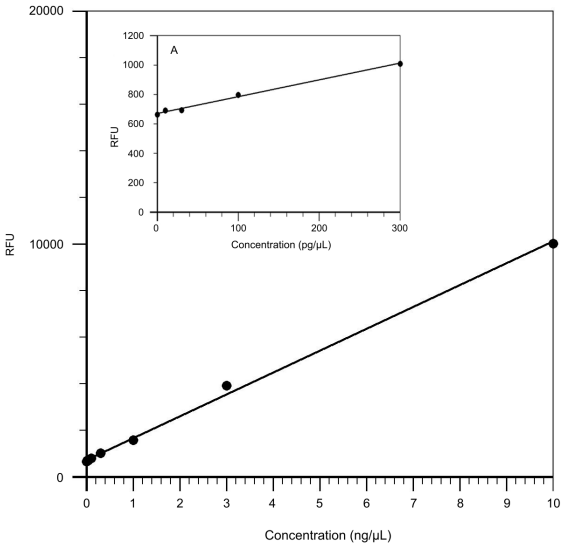


**Figure 3.** The ssDNA standard curve was generated using Portelite™ Fluorimetric ssDNA Quantitation Kit. 0.15 to 10 ng/µL DNA standard dilutions are shown (> 50-fold linear dynamic range). Inset A shows the lower detection limit can extend down to 10 pg.

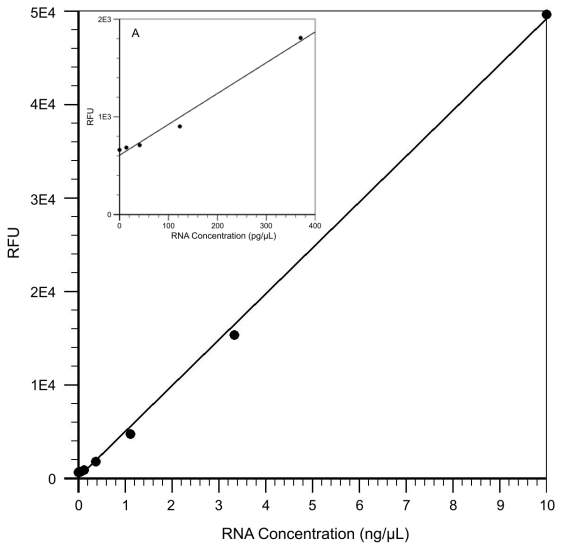


**Figure 4.** The RNA standard curve was generated using Portelite™ Fluorimetric RNA Quantitation Kit. 0.15 to 10 ng/µL RNA standard dilutions are shown (> 50-fold linear dynamic range). Inset A shows the lower detection limit can extend down to 10 pg.

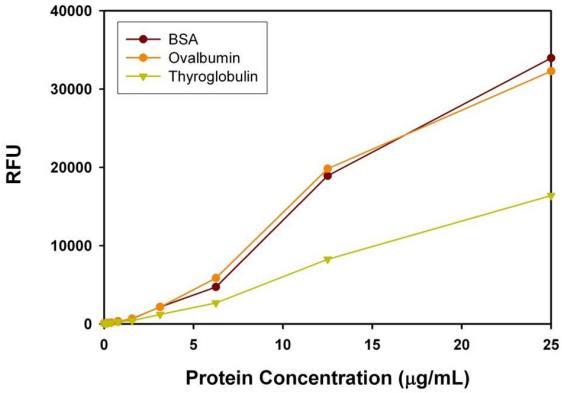


**Figure 5.** Serial dilutions of BSA, chicken-egg ovalbumin, porcine thyroglobulin were measured at Ex/Em = 485/590 nm using the Portelite™ Fluorimetric Protein Quantitation Kit *Optimized for CytoCite™ and Qubit® Fluorometers* with Qubit® Fluorometer. As low as 50 ng/mL of protein can be detected.

yields of in vitro transcribed RNA and measuring RNA concentrations before performing Northern blot analysis, S1 nuclease assays, RNase protection assays, cDNA library preparation, reverse transcription PCR, and differential display PCR. When analyzing gene expression, the amount of the messenger RNA (mRNA) of a gene reveals the level of gene expression. The most commonly used technique for measuring nucleic acid concentration is the determination of absorbance at 260 nm. The absorbance-based method is limited by the interference caused by proteins, free nucleotides, and other UV-absorbing compounds. The use of sensitive and selective fluorescent nucleic acid stains alleviates this interference problem. Portelite™ Fluorimetric RNA Quantitation Kit (17658, 17659) contains the ultrasensitive StrandBrite™ Green Fluorimetric RNA reagent developed for quantifying RNA in solution. The kit detects as little as 5 ng/mL RNA using a CytoCite™ or QubitÒ fluorometer. The Portelite™ Fluorimetric RNA Quantitation Kit includes our StrandBrite™ Green nucleic acid dye, along with an optimized and robust protocol. It provides a convenient method for quantifying RNA in solution.

## Protein Detection

Quantification of protein concentration represents one of the most widely used methods in biomedical research, being particularly applicable to research involving protein extraction, purification, labeling, crystallization, and analysis. Accurate protein quantification is important to a range of other critical assays that require precise results for total protein content in order to generate reliable data. For example, when comparing different protein extracts by SDS-polyacrylamide gel electrophoresis, accurate protein quantitation is necessary to ensure equal amounts of samples are present in each lane. The Portelite™ Fluorimetric Protein Quantitation Kit (11109, 11111) is a rapid and precise fluorescence-based analytical procedure that measures protein concentration in a solution. The assay provides a dynamic range of 12.5 mg/mL to 5 mg/mL when using bovine serum albumin (BSA) as the calibration standard. The kit is more convenient and consumes less precious samples than conventional colorimetric solution assays for protein quantification, such as the bicinchoninic acid (BCA), Bradford (Coomassie Blue), and Lowry assays. The kit is suitable for estimation of protein concentration in measuring protein purity from column fractions after chromatography or samples to be analyzed by electrophoresis, as well as a host of other common research applications. The kit is optimized for performance on the CytoCite™ and Qubit® fluorometers.

### Endotoxin (LPS) Detection

Lipopolysaccharides (LPS), also called endotoxins, are large molecules consisting of a lipid and polysaccharide composed of O-antigen, outer core, and inner core joined by a covalent bond (Dullah and Ongkudon, 2017). Endotoxins are found in the outer membrane of Gram-negative bacteria, and they can bind the CD14/TLR4/MD2 receptor complex in many cell types, particularly in monocytes, dendritic cells, macrophages, and B cells, which subsequently promotes secretion of various pro-inflammatory mediators, leading to septic shock. Detection of contaminating LPS in biopharmaceuticals, particularly protein, peptide, and antibody preparations, is a crucial activity in the context of biomanufacturing and bioprocessing. Portelite™ Rapid Fluorimetric Endotoxin Detection Kit (60008, 60009) uses Endotoxin Green™, a sensitive fluorogenic substrate to detect endotoxin. Endotoxin Green™ is hydrolyzed in the presence of endotoxins and the Limulus Amebocyte Lysate (LAL), an extract of blood cells obtained from horseshoe crabs, to produce a strong green fluorescence signal. The endotoxin activity is proportional to the fluorescence intensity resulting from the hydrolysis of Endotoxin Green™. The kit is optimized for use on CytoCite™ and Qubit® fluorometers and can detect a broad range of endotoxin (from 1 EU/ml to 0.002 EU/ml) present in biological samples.

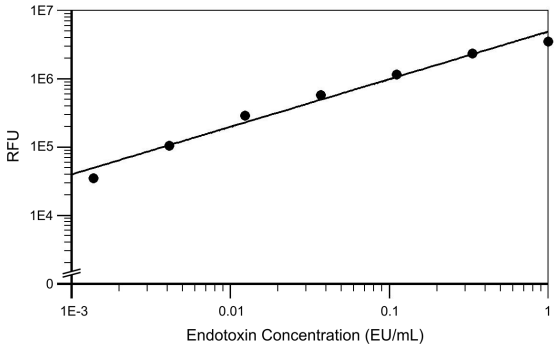


**Figure 6.** *E.coli* endotoxin dose-response was measured in a 0.2 mL, thin-wall PCR tube using the CytoCite™ BG100 in the green fluorescent channel. As low as 0.002 EU/mL of *E.coli* endotoxin can be detected with 10 minutes incubation.

## Conclusion

Compact fluorometers, such as AAT BioQuest's CytoCite™ BG100 and Thermo-Fisher's Qubit® instruments, accurately quantify biological samples, reduce sample consumption requirements and increase assayable dynamic concentration range when compared with conventional cuvette or capillary-based instruments. Compact devices enable the analysis of samples obtained in limited supply, such as material obtained from laser-capture microdissection or needle biopsies. They have also gained popularity when analyzing plentiful sample material due to convenience and minimization of waste disposal requirements. The peak performance of such instruments depends upon the use of optimized fluorescent dyes selective for ssDNA, dsDNA, RNA, total nucleic acid, protein, or endotoxin in order to minimize any impact from sample contaminants on experimental results.

## References

1. Desjardins, P., Conklin, D. NanoDrop microvolume quantitation of nucleic acids. J Vis Exp. 2010

22;(45):2565.
2. Dullah EC, Ongkudon CM. Current trends in endotoxin detection and analysis of endotoxin-protein interactions. Crit Rev Biotechnol. 2017;37(2):251-261
3. Khetan, D., Gupta,N., Chaudhary, R. and Shukla, J.S. Comparison of UV spectrometry and fluorometry-based methods for quantification of cell-free DNA in red cell components. Asian J Transfus Sci. 2019; 13(2): 95–99.
4. Manchester KL (1996) Use of UV methods for measurement of protein and nucleic acid concentrations. Biotechniques 20:968–970.
5. Ponti G, Maccaferri M, Manfredini M, Kaleci S, Mandrioli M, Pellacani G, Ozben T, Depenni R, Bianchi G, Pirola GM, Tomasi A. The value of fluorimetry (Qubit) and spectrophotometry (NanoDrop) in the quantification of cell-free DNA (cfDNA) in malignant melanoma and prostate cancer patients. Clin Chim Acta. 2018;479:14-19.

| Product | Unit Size | Cat No. |
|---|---|---|
| CytoCite™ BG100 Portable Fluorometer | Fluorometer | CBG100 |
| CytoCite™ GR100 Portable Fluorometer | Fluorometer | CGR100 |
| CytoCite™ Sample Tube | 500 Tubes | CCT100 |
| Portelite™ Fluorimetric DNA Quantitation Kit with Broad Dynamic Range *Optimized for Cytocite™ and Qubit® Fluorometers* | 100 Tests | 17665 |
| Portelite™ Fluorimetric High Sensitivity DNA Quantitation Kit *Optimized for CytoCite™ and Qubit® Fluorometers* | 100 Tests | 17660 |
| Portelite™ Fluorimetric High Sensitivity DNA Quantitation Kit *Optimized for CytoCite™ and Qubit® Fluorometers* | 500 Tests | 17661 |
| Portelite™ Fluorimetric Protein Quantitation Kit *Optimized for CytoCite™ and Qubit® Fluorometers* | 100 Tests | 11109 |
| Portelite™ Fluorimetric Protein Quantitation Kit *Optimized for CytoCite™ and Qubit® Fluorometers* | 500 Tests | 11111 |
| Portelite™ Fluorimetric RNA Quantitation Kit*Optimized for Cytocite™ and Qubit® Fluorometers* | 100 Tests | 17658 |
| Portelite™ Fluorimetric RNA Quantitation Kit*Optimized for Cytocite™ and Qubit® Fluorometers* | 500 Tests | 17659 |
| Portelite™ Fluorimetric ssDNA Quantitation Kit *Optimized for Cytocite™ and Qubit® Fluorometers* | 200 Tests | 17625 |
| Portelite™ Fluorimetric Total Nucleic Acid Quantitation Kit *Optimized for Cytocite™ and Qubit® Fluorometers* | 200 Tests | 17631 |
| Portelite™ Rapid Fluorimetric Endotoxin Detection Kit | 50 Tests | 60008 |
| Portelite™ Rapid Fluorimetric Endotoxin Detection Kit | 500 Tests | 60009 |

# Fluorescent Probe Technologies

## Suitable for Multicolor Spectral Flow Cytometry


### *Abstract*

*Flow cytometry is a versatile tool that has applications in numerous biomedical research disciplines, including cancer biology, immunology, infectious disease monitoring, microbiology, and molecular biology. Instrumentation for performing flow cytometry has advanced considerably over the past several decades. Systems incorporating multiple lasers are commonplace, as are specialized instruments designed for particular applications, such as systems using 96-well sample loaders, systems combining microscopy with flow cytometry, and systems combining mass spectrometry with flow cytometry. Spectral flow cytometry measures the entire fluorescence emission spectra for each fluorophore deployed in a multicolor labeling experiment to produce unique spectral fingerprints. Subsequently, each spectrum is unmixed to provide a pure signal for each fluorophore. Such complete spectral analysis is beginning to supplant conventional photomultiplier tube (PMT)-based approaches as the preferred detection approach for high-dimensional multicolor flow cytometry. This technology shift provides an excellent opportunity to implement comprehensive, high-performance fluorophore families spanning the UV-visible-NIR light spectrum.*


## Multicolor Spectral Flow Cytometry Instrumentation

Flow cytometry is an analytical method that provides rapid, multi-parametric analysis of thousands to millions of individual cells in solution (McKinnon, 2018). Particular phenotypic characteristics of individual cells within a cell population are analyzed based upon their fluorescent and light scattering characteristics. Flow cytometry is commonly used in biomedical research and the analysis of clinical specimens. Flow cytometers employ lasers as light sources to generate both scattered and fluorescent signals that are registered by detectors, such as photodiodes or photomultiplier tubes. These analog signals are then converted into electronic signals, analyzed by a computer, and written to a standardized data file format (.fcs).

In order to expand upon the number of fluorophores employed in a flow cytometry experiment beyond ~28, a pretty high level of detail is required to distinguish among fluorophores whose spectral emission signatures are similar. The required level of detail demands high-quality signals, low noise, excitation-specific full emission profiles, and vigilant panel design and optimization. Spectral flow cytometry represents a novel flow cytometry technology platform offering significantly improved multiplexing capabilities relative to traditional flow cytometry (Robinson, 2019; Fox et al., 2020). While in some instances, conventional flow cytometers are capable of detecting panels containing as many as two dozen or so different fluorophores, spectral flow cytometers can distinguish as many as 40 different fluorophores using a single multi-parametric panel.

Spectral flow cytometry shares much of the same hardware that is associated with conventional flow cytometry. Both

systems employ standard fluidic and laser technologies that enable cell-by-cell spectral analysis. For both spectral and conventional flow cytometry methods, the process begins by delivering a sample stream through a flow chamber where cells move in single file at a constant velocity, a process referred to as hydrodynamic focusing. This allows uniform and efficient excitation by a set of monochromatic lasers. Emitted photons are then detected and analyzed by a combination of optics and software to identify unique spectral emission information from fluorophore-labeled biomolecules.

Spectral flow cytometry differs noticeably from traditional flow cytometry when considering its optical configuration and the data analysis software (figure 1). With conventional flow cytometry, photons emitted by a particular fluorophore are directed through a series of dichroic mirrors and bandpass filters to partition the light into a narrow bandwidth for detection by a specific photomultiplier tube (PMT). However, spectral flow cytometry is different in that it employs dispersive optics, such as prisms or spectrographs to disperse photons based upon wavelength across an array of detectors. This approach broadens a fluorophore's spectral profile by capturing the entire visible and near-IR spectrum of light, allowing for higher resolution spectral analysis relative to the aforementioned traditional optical configurations, which detect only a tiny portion of the emission spectra. As a result, fluorophores with similar emission spectral profiles that are challenging to differentiate by traditional flow cytometry can readily be distinguished using spectral flow cytometry. As many as 40 different fluorophores can be analyzed, including those with emission spectra in close proximity to one other.

Despite its superior ability to distinguish between fluorophores, it is advisable to use fundamental flow cytometry principles in panel construction and avoid spectral spillover where possible when designing spectral flow cytometry experiments. Designing robust multicolor fluorescence panels entails vigilant consideration of fluorophore spectral properties,

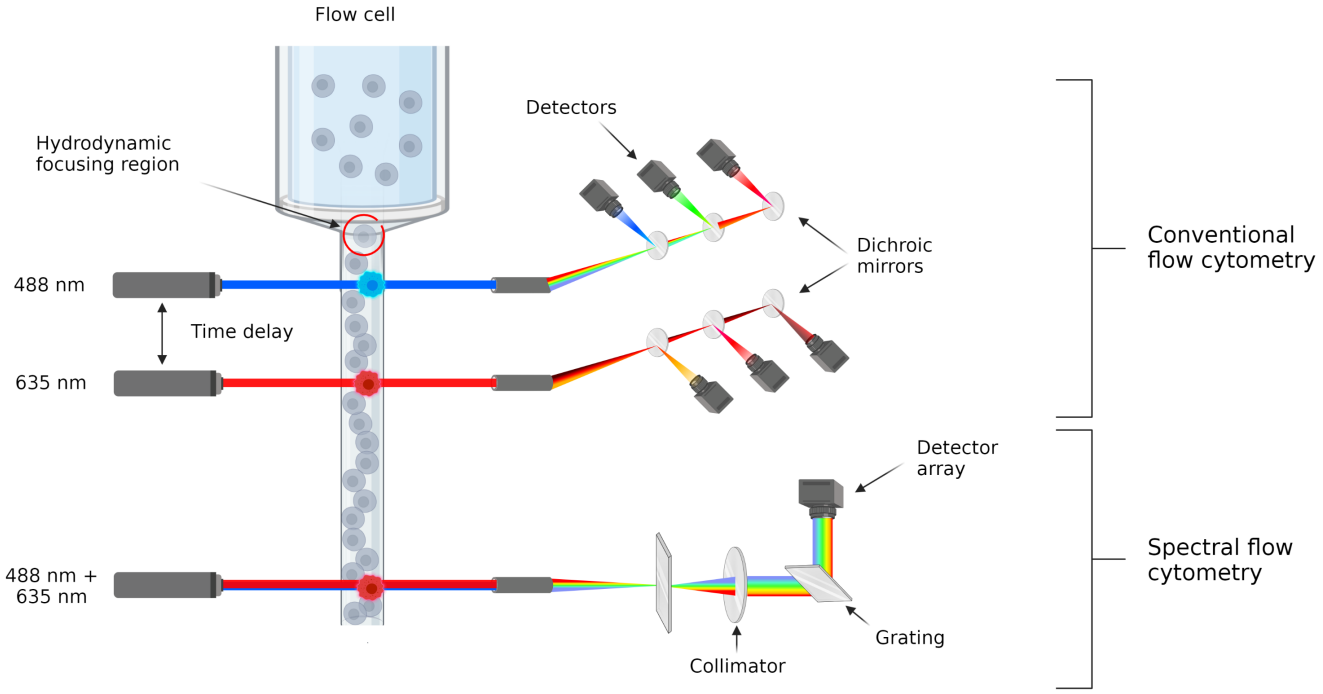


**Figure 1. Comparison of conventional and spectral flow cytometer systems.** (Top) A conventional flow cytometer relies on a series of bandpass filters and dichroic mirrors to separate light emissions into individual detectors. (Bottom) A spectral flow cytometer uses a grating or prism element to separate light into a focusing lens prior to detection. As separating light keeps diverging in space, a collimating lens is often used to parallelize and direct light linearly before reaching a detector.

choosing those spectral profiles that are best separated by the instrument. Using traditional flow cytometry, any multi-parametric panel containing a dozen or more fluorophores will undoubtedly have some overlap of emission spectra, resulting in noise in channels from emissions of unintended fluorophores (i.e., spectral spillover). To account for this, single-color control samples must be included with each experiment to ascertain the level of spectral overlap encountered in each detector. Then, with traditional flow cytometry, a mathematical approach referred to as compensation is applied using the controls to subtract overlapping spectra and effectively isolate a fluorophore's emission profile. This is achieved with a correction factor obtained using the ratio of the intended and unintended fluorophores emitting into a particular channel.

Mathematical models are required with spectral flow cytometry to correct for any spectral spillover among channels. This is necessary since the instrument must distinguish between multiple fluorescent profiles across the entire visible light spectrum rather than from a few distinct channels. The process of deconvoluting fluorophore emission spectra across an array of detectors is known as spectral unmixing. This form of compensation also requires experimental reference controls as well as noise-reducing mathematical algorithms, such as the least-squares method. This approach is especially valuable when interrogating cell culture samples, which are susceptible to a high degree of autofluorescence.

The Cytek Aurora benchtop flow cytometer (Fremont, CA) is a high-performance spectral flow cytometer that the AAT Bioquest team has extensive experience using in conjunction with our comprehensive suite of fluorophores and fluorescent proteins. The instrument leverages full-spectrum technology to enable the use of a wide range of novel fluorophore combinations without reconfiguring the system for each application. The instrument generates high-resolution data at the single-cell level, facilitating the resolution of even the most challenging cell populations, including cells exhibiting high autofluorescence or cells expressing low levels of target biomarkers, even in the context of complex multi-analyte detection. Their SpectroFlo® software provides an intuitive workflow that guides users from QC to data analysis with tools that simplify performing even the most challenging applications.

With up to five lasers, three scattering channels, and 64 fluorescence channels, the Aurora system is highly flexible, intuitive, and ultra-sensitive. With its intuitive optical design, compact footprint, and upgradeability from 3 to 5 laser configurations, the Aurora system suits every laboratory's needs, from simple to high complexity applications.

The system's state-of-the-art optics and low-noise electronics provide excellent sensitivity and resolution. Flat-top beam profiles, combined with a uniquely designed fluidics system, translate to outstanding instrument performance, even at high sample flow rates.

## Optimized Multicolor Immunofluorescence Panels for Multicolor Spectral Flow Cytometry

A wide range of fluorescent reagents is employed in flow cytometry, including fluorescent dye-conjugated antibodies, DNA binding dyes, viability dyes, ion indicator dyes, and different fluorescent proteins. By collecting substantially more

**Table 1.** Comparison between traditional and spectral flow cytometry.

| Parameter | Conventional Flow Cytometry | Spectral Flow Cytometry |
|---|---|---|
| **Optical Hardware** | Bandpass filters & dichroic mirrors<br>Captures a narrow portion of a fluorophore's emission spectrum | Dispersive optics capture entire fluorophore's emission spectrum |
| **Spectral Resolution** | Acquires a narrow emission bandwidth from a single-laser excitation source | Acquires the entire fluorophore emission profile for each laser excitation source |
| **Fluorophore Separation** | Achieved by compensation (loss of some acquisition data) | Achieved by spectral unmixing (preserves more acquisition data) |
| **Detection Sensitivity** | Detection sensitivity is compromised by using compensation to address signal spill over | Superior detection sensitivity is assured using state-of-the-art optics and low noise electronics |
| **Multiplexing Capability** | Limited to perhaps 12 due to spectral overlap of fluorophores & limited number of detectors/filters installed in instrument | Superior spectral resolution so that as many as 40 fluorophore probes can be employed in a single analysis |

information than conventional flow cytometry concerning each cell in a sample, full-spectrum multicolor flow cytometry has become the platform of choice for developing optimized multicolor immunofluorescence panels (OMIPs). Numerous OMIPs have been published in the literature over the years, obviating the need for extensive time to independently design such panels (Mahnke et al., 2010; Park et al., 2020). These published OMIPs also serve as valuable starting points for creating novel OMIPs and provide a mechanism for recognizing panel developers through citation of their work.

As an impressive example of a biomedical research problem requiring the application of OMIPs, elucidating the intricate details of the human immune response requires the capacity to perform high-throughput, in-depth analysis at both the single-cell and population levels. OMIP-069 is a recently developed forty-color full spectrum flow cytometry panel designed for the deep immunophenotyping of major cell subsets in human peripheral blood, including subsets of T, B, NK, NKT, monocyte, and dendritic cells (Park et al., 2020). The cited panel shares similarities with OMIPs -015, -023, -024, -030, -033, -034, -042, -50, -058, -063, which were designed to identify the major leukocyte subsets in human blood, but also partially overlaps with OMIPs -013, -017, -021, -030, and -060 to facilitate characterization of T cells; OMIPs -004, -006, and -015 for Treg immunophenotyping; OMIP -044 for dendritic cells; OMIPs-003, -033, and -051 for B cells; and OMIPs -029, and -039 for NK cells. The panel includes a live-dead viability stain, a compendium of organic fluorophores, and various fluorescent proteins, such as allophycocyanin (APC), peridinin-chlorophyll-protein (PerCP), and various phycoerythrin (PE)-dye conjugates. The cited 40-color panel provides a potent approach for the in-depth characterization of lymphocytes, monocytes, and dendritic cells in human peripheral blood. The panel is suitable for interrogating nearly the entire cellular composition of the human peripheral immune system and should be particularly valuable for studies wherein sample availability is limited or unique biomarker signatures are being pursued.

## Selecting Fluorophores for the Development of Multicolor Phenotypic Panels

In flow cytometry methods development, it is critically important to be familiar with the configuration of the instrument that a particular phenotypic panel is being designed for. The number and types of lasers and filters that the instrument is equipped with dictate which fluorophores can be deployed in the panel. Fluorophores are selected that have excitation maxima closely matching the lasers in the system, while for conventional flow cytometry filters should be designed to detect the targeted fluorophore's emission wavelength maximum without registering light from other laser sources in the instrument. For multicolor spectral flow cytometry, an entire emission profile is detected, and fluorophores should be readily distinguishable on this basis. Typically, when a panel of fluorophores is required, distributing fluorophores as widely as possible across the excitation and emission spectra are recommended to minimize interference.

To minimize any signal spillover, which can adversely influence resolution and sensitivity, bright fluorophores, such as PE and APC, should be used with low abundance phenotypic

**Table 2.** Comparison between traditional and spectral flow cytometry.

| Panel | Plex | Target | Citation |
|---|---|---|---|
| **OMIP-020** | **12** | Phenotypic characterization of human γδT-cells | Wistuba-Hamprecht et al., 2014 |
| **OMIP-037** | **16** | Measuring inhibitory receptor signatures from multiple human immune cell subsets | Belkina et al., 2017 |
| **OMIP-041** | **9** | Phenotypic characterization of rat-derived microglial cells isolated from brain or spinal cord | Toledano Furman et al., 2018 |
| **OMIP-050** | **28** | Enumerating and characterizing cells expressing a wide array of immune checkpoint molecules | Nettey et al., 2018 |
| **OMIP-069** | **40** | Deep immunophenotyping of major cell subsets in human peripheral blood | Park et al., 2020 |
| **OMIP-070** | **27** | Deep immunophenotyping of major cell subsets in human peripheral blood | Frutoso et al., 2020 |

targets, and organic fluorophores, such as mFluor™ dyes should be paired with more highly expressed targets. This improves the ability of the flow cytometer to discriminate between specific signal and background fluorescence arising from variables such as non-specific staining and cellular autofluorescence. In cases wherein an antibody is not commercially available bound to the desired fluorophore, ATT Bioquest offers custom antibody labeling kits and services.

## The mFluor™ Dyes

As briefly summarized above, the foundation for developing multicolor phenotypic panels, such as the OMIPs, is a high-performance series of reactive organic fluorophores, fluorescent proteins, and tandem fluorophore-fluorescent protein conjugates that span the UV to near-infrared (NIR) region of the light spectrum. Designing and optimizing these panels can be a time-consuming and challenging activity. Several hurdles must be overcome, such as qualification (e.g., titration) of individual reagents, evaluating any potential interactions between reagents selected for a particular panel, choosing the best combination of fluorophore-antibody pairings, and overcoming the sensitivity losses inherent in multicolor fluorescence experiments. The design and optimization phase of creating even a modest 12 color panel may require 2–4 months of effort before the panel is mature enough for actual experimental applications. As a dedicated vendor in this specialized area of reagents, AAT Bioquest offers in-house developed conjugates, including custom-synthesized conjugates, to assist investigators in achieving the high-level multiplexing required for the development of multicolor immunofluorescence panels.

Developed exclusively by AAT Bioquest, mFluor™ dyes

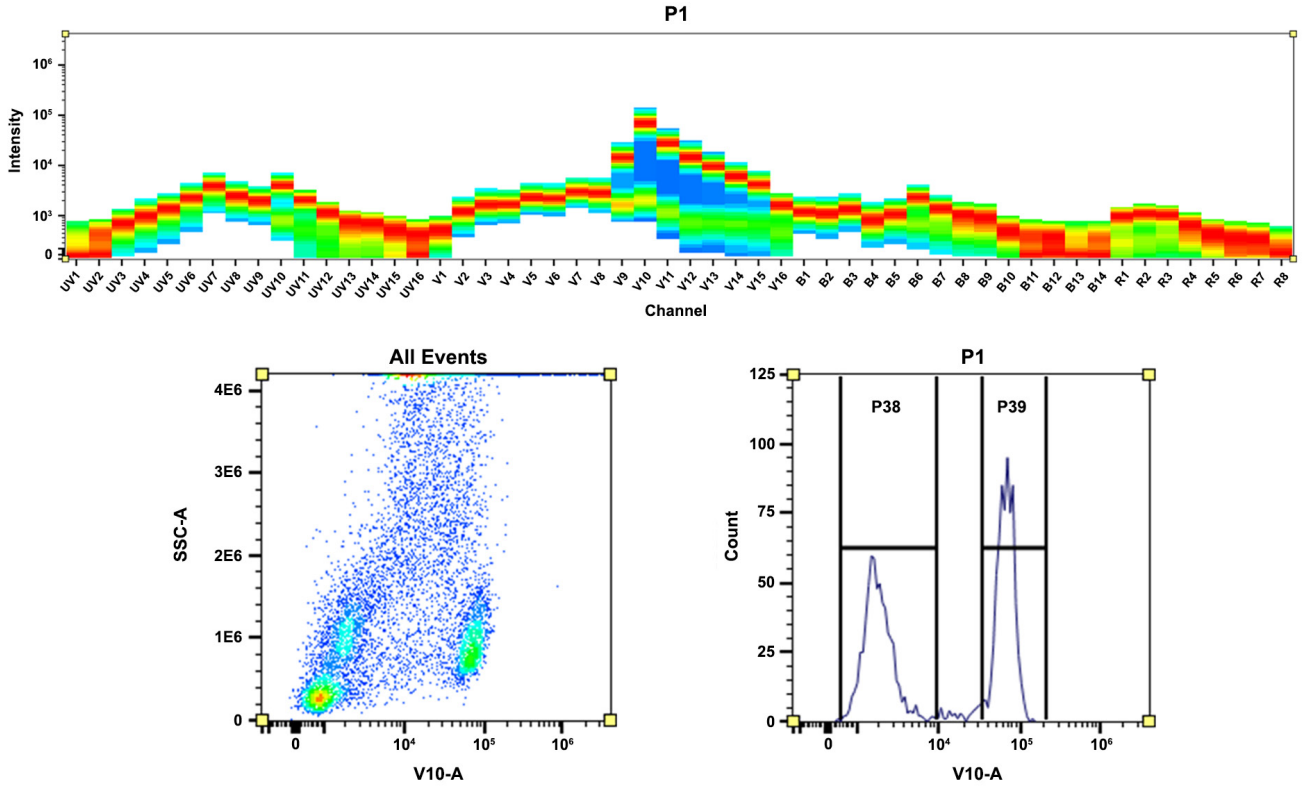


**Figure 2.** (Top) Spectral pattern was generated using a 4-laser spectral cytometer. Spatially offset lasers (355 nm, 405 nm, 488 nm, and 640 nm) were used to generate four distinct emission profiles, then, when combined, yielded the overall spectral signature. Bottom) Flow cytometry analysis of whole blood cells stained with CD4-mFluor™ Violet 610 conjugate. The fluorescence signal was monitored using a Cytek® Aurora flow cytometer in the mFluor™ Violet 610 specific V10-A channel.

exhibit excellent aqueous solubility and large Stokes Shifts, and their hydrophilic nature minimizes the need for employing organic solvents (Table 3). Currently, we offer 26 unique mFluor™ SE dyes. mFluor™ dyes use the following naming convention: 'mFluor™ + Excitation Laser + Emission Wavelength + Reactivity'. For example, mFluor™ UV460 SE (Ex/Em max = 364/461) is a UV light-excitable succinimidyl ester dye that emits around 460 nm.

mFluor™ dyes have been used extensively to label antibodies proteins and other biomolecules for multicolor flow cytometry applications. The absorbance maxima of mFluor™ dyes are designed to be optimally excited by one of the major laser lines commonly equipped in flow cytometers, such as the 350 nm, 405 nm, 488 nm, 532 nm, 561-568 nm, or 633-647 nm laser lines. In conjunction with phycobiliproteins PE, APC, and their tandems, mFluor™ dyes are excellent fluorophores for immunophenotyping (figure 2), FACS, and other flow cytometry-based applications. mFluor™ dyes are available in a wide selection of products, including reactive dyes and antibody labeling kits, as well as mFluor™ streptavidin conjugates for signal amplification and annexin V-mFluor™ conjugates for apoptosis detection.

One crucial advantage of mFluor™ reactive dyes is that they can be covalently labeled to biomolecules without self-quenching, which results in intensely bright fluorescent

**Table 3.** mFluor™ active esters and kits for labeling antibodies, proteins and amine-modified biomolecules..

| mFluor™ Dye | Laser | Ex max | Em max | ε[1] | Φ[2] | CF @260 | CF @280 | Succinimidyl Ester | ReadiLink™ Kits |
|---|---|---|---|---|---|---|---|---|---|
| mFluor™ UV375 | UV | 351 | 387 | 30,000 | 0.94 | 0.099 | 0.138 | 1135 | |
| mFluor™ UV420 | UV | 353 | 421 | 80,000 | | | | 1641 | |
| mFluor™ UV455 | UV | 357 | 461 | 20,000 | 0.42 | 0.651 | 0.406 | 1642 | |
| mFluor™ UV460 | UV | 358 | 456 | 15,000 | 0.86 | 0.35 | 0.134 | 1136 | |
| mFluor™ UV520 | UV | 370 | 524 | 80,000 | 0.03 | 0.495 | 0.518 | 1643 | |
| mFluor™ UV540 | UV | 373 | 560 | 90,000 | 0.35 | 0.634 | 0.463 | 1645 | |
| mFluor™ UV610 | UV | 371 | 609 | 90,000 | 0.25 | 0.949 | 0.904 | 1649 | |
| mFluor™ Violet 420 | Violet | 403 | 427 | 37,000 | 0.91 | | | | 1105 |
| mFluor™ Violet 450 | Violet | 406 | 445 | 35,000 | 0.81 | 0.338 | 0.078 | 1150 | 1100 |
| mFluor™ Violet 500 | Violet | 410 | 501 | 25,000 | 0.81 | 0.769 | 0.365 | 1149 | |
| mFluor™ Violet 505 | Violet | 393 | 504 | 40,000 | 0.45 | 0.888 | 0.403 | 1154 | |
| mFluor™ Violet 510 | Violet | 412 | 505 | 25,000 | 0.86 | 0.464 | 0.366 | 1151 | 1110 |
| mFluor™ Violet 540 | Violet | 402 | 535 | 18,000 | 0.21 | 1.326 | 0.543 | 1152 | 1114 |
| mFluor™ Violet 545 | Violet | 393 | 543 | 20,000 | 0.15 | 1.080 | 0.496 | 1157 | |
| mFluor™ Violet 550 | Violet | 419 | 550 | 90,000 | 0.31 | 0.474 | 0.306 | 1153 | |
| mFluor™ Violet 590 | Violet | 424 | 591 | 90,000 | 0.22 | 0.632 | 0.329 | 1155 | |
| mFluor™ Violet 610 | Violet | 421 | 613z | 92,000 | 0.3 | 0.532 | 0.660 | 1156 | |
| mFluor™ Blue 570 | Blue | 503 | 565 | 120,000 | 0.08 | 0.228 | 0.179 | 1160 | 1120 |
| mFluor™ Blue 580 | Blue | 485 | 580 | 40,000 | 0.02 | 0.363 | 0.247 | 1178 | |
| mFluor™ Blue 590 | Blue | 500 | 589 | 81,000 | 0.15 | 0.671 | 0.406 | 1161 | |
| mFluor™ Blue 620 | Blue | 500 | 616 | 98,000 | 0.18 | 0.683 | 0.849 | 1163 | |
| mFluor™ Blue 630 | Blue | 470 | 634 | 49,000 | 0.015 | 0.197 | 0.275 | 1164 | |
| mFluor™ Blue 660 | Blue | 481 | 663 | 26,000 | | 0.338 | 0.320 | 1180 | |
| mFluor™ Green 620 | Blue/Green | 525 | 623 | 50,000 | 0.06 | 0.895 | 0.569 | 1165 | 1123 |
| mFluor™ Green 630 | Blue/Green | 537 | 657 | 51,000 | | | | 1168 | |
| mFluor™ Yellow 630 | Green/Yellow | 570 | 632 | 110,000 | 0.01 | 0.283 | 0.413 | 1170 | 1126 |
| mFluor™ Red 700 | Red | 633 | 695 | 295,000 | 0.029 | 0.135 | 0.127 | 1190 | 1130 |
| **mFluor™ Red 780** | **Red** | 629 | 767 | 90,000 | 0.034 | 0.101 | 0.116 | 1191 | 1131 |

conjugates. mFluor™ reactive dye formats include amine-reactive succinimidyl esters (SE) and thiol-reactive maleimides for labeling antibodies and proteins. Additionally, mFluor™ dyes are available as their acid form for labeling proteins, peptides, amine-modified oligonucleotides, and other amine-containing biomolecules using carbodiimide conjugation chemistry (EDAC).

To ensure stable, dependable antibody labeling for a variety of flow cytometry applications, antibody labeling kits can be an optimum choice for preparing the required antibody conjugates. ReadiLink™ Rapid mFluor™ Antibody Labeling Kits from AAT Bioquest provide a convenient method for labeling microscale volumes of antibodies with our superior mFluor™ dyes. The unique chemistry of ReadiLink™ kits enables researchers to effortlessly label and recover 100% of their antibodies without a purification step. Since ReadiLink™ mFluor™ conjugates are covalently labeled, they are stable for long-term storage and are ideal for demanding applications including immunophenotyping, multiplex flow cytometry, FACS, and other flow-based applications. Also available are ReadiLink™ Rapid and xtra Rapid Antibody Labeling kits for conjugation of mFluor™ dyes, Alexa Fluor® dyes, other fluorescent dyes, biotin, BSA, and KLH.

mFluor™ dyes provide simple, quick, and robust labeling of biomolecules, with high conjugation yields. The fluorophores offer superior photostability, solubility, and brightness generating strong fluorescence emissions over a broad pH range with little pH sensitivity and low spillover into most PMT detectors. As such, mFluor™ dyes offer excellent choices and flexibility for the design of multicolor phenotypic panels. Learn more about mFluor™ dyes at **aatbio.com/catalog/mfluor-dyes-and-kits.**

## Phycobiliproteins

Phycobiliproteins are photosynthetic light-harvesting proteins obtained from microalgae and cyanobacteria. This family of proteins contains covalently attached linear tetrapyrrole groups, referred to as phycobilins, which are involved in capturing light energy. In nature, energy absorbed by these phycobilins is efficiently transferred, by the process of fluorescence resonance energy transfer (FRET), to chlorophyll pigments for use in the photosynthetic process. Since phycobiliproteins possess extremely high fluorescence quantum yields and absorbance coefficients (e.g., molar extinction coefficients) over a wide range of the light spectrum, they are exceedingly fluorescent and thus are considered an excellent reagent for use in fluorescence applications, especially in flow cytometry (Table 4).

Phycoerythrin (PE), allophycocyanin (APC), and their tandem fluorophore conjugates are among the most suitable phycobiliproteins for flow cytometry applications. Conjugation of these dyes to macromolecules with biological specificities, such as antibodies, protein A or streptavidin, can be used in fluorescence-based detection applications that require high sensitivity but not necessarily photostability, such as fluorescence-activated cell sorting (FACS) and immunophenotyping. Compared with organic and synthetic fluorescent dyes, the advantages of phycobiliproteins as fluorescent labels include; long-wavelength fluorescence excitation and emission to minimize interference by auto-fluorescence from biological materials, minimal fluorescence quenching, high water-solubility, significant Stokes shifts with well-resolved emission spectra for multicolor analysis and multiple sites providing for stable conjugation with organic and synthetic compounds, including antibodies, cyanine dyes, iFluor™ dyes, and mFluor™ dyes. Learn more at **aatbio.com/catalog/pe-and-apc.**

## Tandem Dyes Further Expand Options for Multicolor Immunofluorescence Panels

When developing high-plex phenotypic panels, the use of spectrally similar fluorophores becomes practically unavoidable. One solution to this problem is to separate the complex fluorophore combinations by segregating them into cellular subpopulations that are gated and analyzed separately, thus limiting spectral spillover between populations. Another helpful approach for increasing panel size and diversity is by employing tandem dyes.

Tandem dyes comprise of two different fluorophores, a fluorescent donor and a longer-wavelength emitting

**Table 4.** PE, APC, and tandem dyes and kits for labeling antibodies, proteins, and other biomolecules.

| Phycobiliprotein | Laser | Ex max | Em max | Dye/Tandem[1] | ReadiUse™ Dye/Tandem[2] | Buccutite™ Antibody Labeling Kit |
|---|---|---|---|---|---|---|
| Phycoerythrin (PE) | Blue/Green/Yellow | 495, 546, 566 | 574 | 2558 (1 mg)<br>2556 (10 mg)<br>2557 (100 mg) | 2500 (1 mg)<br>2501 (10 mg) | 1312 (labels 25 µg Ab/reaction)<br>1310 (labels 100 µg Ab/reaction) |
| PE-iFluor™ 594 | Blue/Green/Yellow | 495, 546, 566 | 606 | 2600 | 2584 | |
| PE-Texas Red | Blue/Green/Yellow | 495, 546, 566 | 615 | 2619 | 2583 | 1343 (labels 25 µg Ab/reaction)<br>1318 (labels 100 µg Ab/reaction) |
| PE-iFluor™ 610 | Blue/Green/Yellow | 495, 546, 566 | 625 | 2700 | | |
| PE-iFluor™ 647 | Blue/Green/Yellow | 495, 546, 566 | 666 | 2702 | 2577 | |
| PE-Cy5 | Blue/Green/Yellow | 495, 546, 566 | 666 | 2610 | 2580 | 1340 (labels 25 µg Ab/reaction)<br>1322 (labels 100 µg Ab/reaction) |
| PE-Cy5.5 | Blue/Green/Yellow | 495, 546, 566 | 671 | 2613 | 2581 | 1341 (labels 25 µg Ab/reaction)<br>1316 (labels 100 µg Ab/reaction) |
| PE-iFluor™ 660 | Blue/Green/Yellow | 495, 546, 566 | 695 | 2602 | 2579 | |
| PE-iFluor™ 700 | Blue/Green/Yellow | 495, 546, 566 | 708 | 2614 | 2585 | |
| PE-iFluor™ 710 | Blue/Green/Yellow | 495, 546, 566 | 740 | 2615 | | |
| PE-iFluor™ 750 | Blue/Green/Yellow | 495, 546, 566 | 778 | 2704 | 2578 | |
| PE-Cy7 | Blue/Green/Yellow | 495, 546, 566 | 778 | 2616 | 2582 | 1342 (labels 25 µg Ab/reaction)<br>1317 (labels 100 µg Ab/reaction) |
| Allophycocyanin (APC) | Red | 651 | 660 | 2554 (1 mg)<br>2555 (10 mg) | 2561 | 1313 (labels 25 µg Ab/reaction)<br>1311 (labels 100 µg Ab/reaction) |
| Cross-linked Allophycocyanin (CL-APC) | Red | 651 | 660 | 2552 (1 mg)<br>2549 (10 mg)<br>2550 (50 mg)<br>2551 (100 mg) | 2503 (1 mg)<br>2504 (10 mg) | |
| APC-Cy5.5 | Red | 651 | 700 | 2622 | 2586 | 1350 (labels 25 µg Ab/reaction)<br>1320 (labels 100 µg Ab/reaction) |
| APC-XFD700 | Red | 651 | 707 | 2624 | | |
| APC-iFluor™ 700 | Red | 651 | 710 | 2623 | 2570 | 1347 (labels 25 µg Ab/reaction)<br>1319 (labels 100 µg Ab/reaction) |
| APC-Cy7 | Red | 651 | 779 | 2625 | 2587 | 1351 (labels 25 µg Ab/reaction)<br>1321 (labels 100 µg Ab/reaction) |
| APC-XFD750 | Red | 651 | 782 | 2627 | | |
| APC-iFluor™ 750 | Red | 651 | 793 | 2626 | 2571 | |
| APC-iFluor™ 800 | Red | 651 | 819 | 2630 | 2572 | |

fluorescence acceptor, that are conjugated to the same biomolecule. One fluorophore in the pair transmits energy to the other by the process of fluorescence resonance energy transfer (FRET). Since the second fluorophore emits light at a higher wavelength than that emitted by the first fluorophore, the number of fluorophores that can be distinguished using the same laser for excitation is effectively increased. Typically, PE and APC are used as donor fluorophores when generating tandem dyes, as illustrated with APC-iFluor™ 700 and PE-iFluor™ 750. In flow cytometry, tandem dyes are particularly suited for multicolor analysis of cells due to their exploitation of a single excitation source and their significantly large Stokes shifts.

PerCP (Peridinin-chlorophyll-protein complex), obtained from Dinophyceae spinosum, has an extremely high extinction coefficient, a high quantum efficiency, and a large Stokes shift. It is especially well excited by the 488 nm argon-ion laser, with its maximum emission peak at 677 nm. PerCP protein is commonly employed for fluorescent immunolabeling, especially fluorescent-activated cell sorting (FACS). Tandem conjugates with cyanine dyes, such as PerCP-Cy5.5, can be excited with

a standard 488 nm laser and emits in the far red at a longer wavelength for multicolor flow cytometric analysis of cells. These multiple emission wavelengths make PerCP-cyanine conjugates potentially useful fluorochromes for multicolor analysis with FITC, PE, and other fluorophores. AAT Bioquest offers iFluor™ and mFluor™ protein labeling dyes, which are generally brighter and more photostable than the corresponding cyanine dyes of similar wavelengths.

## Conclusion

The requirement to simultaneously interrogate increasingly more phenotypic features in complex cell populations, such as human peripheral blood cells, has demanded the implementation of more powerful instrumentation adaptations beyond those found in traditional flow cytometry. One important advance in multicolor immunofluorescence analysis has been the introduction of full spectrum multicolor spectral flow cytometry. This technology captures the entire emission spectrum of fluorophores using arrays of highly sensitive light detectors and has enabled simultaneous characterization of as many as 40 parameters in a single sample (Park et al., 2020). Implementation and broad adoption of this new flow cytometry-based instrumentation require careful design and validation of optimized multicolor immunofluorescence panels (OMIPs). These, in turn, require the availability of high-performance series of reactive organic fluorophores, fluorescent proteins, and tandem fluorophore-fluorescent protein conjugates that span the UV-visible-NIR region of the light spectrum.

## References


1. Belkina AC, Snyder-Cappione JE. OMIP-037: 16-color panel to measure inhibitory receptor signatures from multiple human immune cell subsets. Cytometry A. 2017 Feb;91(2):175-179. doi: 10.1002/cyto.a.22983.
2. Fox A, Dutt TS, Karger B, Obregon-Henao A, Anderson GB, Henao-Tamayo M. Acquisition of High-Quality Spectral Flow Cytometry Data. Curr Protoc Cytom. 2020 Jun;93(1):e74.
3. Frutoso M, Mair F, Prlic M. OMIP-070: NKp46-Based 27-Color Phenotyping to Define Natural Killer Cells Isolated From Human Tumor Tissues. Cytometry A. 2020 Oct;97(10):1052-1056. doi: 10.1002/cyto.a.24230.
4. Mahnke Y, Chattopadhyay P, Roederer M. Publication of optimized multicolor immunofluorescence panels. Cytometry A. 2010 Sep;77(9):814-8. doi: 10.1002/cyto.a.20916.
5. McKinnon KM. Flow Cytometry: An Overview. Curr Protoc Immunol. 2018 Feb 21;120:5.1.1-5.1.11. doi: 10.1002/cpim.40.
6. Nettey L, Giles AJ, Chattopadhyay PK. OMIP-050: A 28-color/30-parameter Fluorescence Flow Cytometry Panel to Enumerate and Characterize Cells Expressing a Wide Array of Immune Checkpoint Molecules. Cytometry A. 2018 Nov;93(11):1094-1096. doi: 10.1002/cyto.a.23608.
7. Park LM, Lannigan J, Jaimes MC. OMIP-069: Forty-Color Full Spectrum Flow Cytometry Panel for Deep Immunophenotyping of Major Cell Subsets in Human Peripheral Blood. Cytometry A. 2020 Oct;97(10):1044-1051. doi: 10.1002/


## 24-Color panel for identifying circulating cell subsets in human peripheral blood

| Specificity | Violet Laser Fluorochromes | Specificity | Blue Laser Fluorochromes | Specificity | Red Laser Fluorochromes |
|---|---|---|---|---|---|
| CCR7 | mFluor™ Violet 420 | CD11c | XFD488 (Alexa Fluor® 488 Equivalent) | CD27 | APC |
| CD19 | mFluor™ UV420 | CD45RA | iFluor™ 488 | CD123 | iFluor™ 647 |
| CD16 | mFluor™ Violet 450 | CD3 | iFluor™ 532 | CD127 | APC-iFluor™ 700 |
| TCR gamma delta | mFluor™ Violet 500 | CD25 | PE | HLA DR | APC-iFluor™ 750 |
| CD14 | mFluor™ Violet 510 | IgD | PE-iFluor™ 594 | | |
| CD8 | mFluor™ Violet 590 | CD95 | PE-Cy5 | | |
| CD1c | mFluor™ Violet 610 | CD11b | PerCP-Cy5.5 | | |
| PD-1 | Brilliant Violet 650™ | CD38 | PerCP-eFluor® 710 | | |
| CD56 | Brilliant Violet 711™ | CD57 | PE-Cy7 | | |
| CD4 | Brilliant Violet 750™ | | | | |
| CD28 | Brilliant Violet 785™ | | | | |

cyto.a.24213.
8. Robinson JP. Spectral flow cytometry-Quo vadimus? Cytometry A. 2019 Aug;95(8):823-824. doi: 10.1002/cyto.a.23779. Epub 2019 Apr 30. PMID: 31038271.
9. Toledano Furman NE, Prabhakara KS, Bedi S, Cox CS Jr, Olson SD. OMIP-041: Optimized multicolor immunofluorescence panel rat microglial staining protocol. Cytometry A. 2018 Feb;93(2):182-185. doi: 10.1002/cyto.a.23267.
10. Wistuba-Hamprecht K, Pawelec G, Derhovanessian E. OMIP-020: phenotypic characterization of human gamma delta T-cells by multicolor flow cytometry. Cytometry A. 2014 Jun;85(6):522-4. doi: 10.1002/cyto.a.22470.

| Product | Unit Size | Cat No. |
|---|---|---|
| CCR7 Antibody | 50 ug | 8G053 |
| Purified Mouse Anti-human/pig HLA-DR/DP Antibody *HL-40, monoclonal* | 0.1 mg | V1031000 |
| Purified Mouse Anti-human HLA-DR/DP Antibody *MEM-136, monoclonal* | 0.1 mg | V1031005 |
| Purified Mouse Anti-human IgD Antibody *IA6-2, monoclonal* | 0.1 mg | V1031415 |
| Purified Mouse Anti-human TCR α/β Antibody *IP26, monoclonal* | 0.1 mg | V1032215 |
| Purified Mouse Anti-non-human primates/rat TCR α/β Antibody *R73, monoclonal* | 0.1 mg | V1032220 |
| Purified Low Endotoxin Mouse Anti-non-human primates/rat TCR α/β Antibody *R73, monoclonal* | 0.1 mg | V1032225 |
| Purified Mouse Anti-human/non-human primates TCR γ/δ Antibody *B1, monoclonal* | 0.1 mg | V1032265 |
| Purified Mouse Anti-rat TCR γ/δ Antibody *V65, monoclonalδ* | 0.1 mg | V1032270 |
| Purified Low Endotoxin Mouse Anti-human/non-human primates TCR γ/δ Antibody *B1, monoclonal* | 0.1 mg | V1032275 |
| Purified Azide Free Mouse Anti-human TCR Vβ5.3-related Antibody *MEM-262, monoclonal* | 0.1 mg | V1032305 |
| Purified Mouse Anti-human TCR Vβ5.3-related Antibody *MEM-262, monoclonal* | 0.1 mg | V1032310 |
| Purified Low Endotoxin Mouse Anti-human TCR Vβ5.3-related Antibody *MEM-262, monoclonal* | 0.1 mg | V1032315 |
| Purified Mouse Anti-human HLA-DR Antibody *HL-39, monoclonal* | 0.1 mg | V103915 |
| Purified Mouse Anti-human HLA-DR Antibody *MEM-12, monoclonal* | 0.1 mg | V103920 |
| Purified Mouse Anti-human/dog/non-human primates HLA-DR Antibody *L243, monoclonal* | 0.1 mg | V103925 |
| Purified Low Endotoxin Mouse Anti-human/dog/non-human primates HLA-DR Antibody *L243, monoclonal* | 0.1 mg | V103930 |
| Purified Mouse Anti-human/pig HLA-DR/DP Antibody *HL-38, monoclonal* | 0.1 mg | V103995 |
| ReadiLink™ Rapid mFluor™ Violet 450 Antibody Labeling Kit *Microscale Optimized for Labeling 50 µg Antibody Per Reaction* | 2 Labelings | 1100 |
| ReadiLink™ Rapid mFluor™ Violet 420 Antibody Labeling Kit *Microscale Optimized for Labeling 50 µg Antibody Per Reaction* | 2 Labelings | 1105 |
| ReadiLink™ Rapid mFluor™ Violet 510 Antibody Labeling Kit *Microscale Optimized for Labeling 50 µg Antibody Per Reaction* | 2 Labelings | 1110 |
| ReadiLink™ Rapid mFluor™ Violet 540 Antibody Labeling Kit *Microscale Optimized for Labeling 50 µg Antibody Per Reaction* | 2 Labelings | 1114 |
| ReadiLink™ Rapid mFluor™ Blue 570 Antibody Labeling Kit *Microscale Optimized for Labeling 50 µg Antibody Per Reaction* | 2 Labelings | 1120 |
| ReadiLink™ Rapid mFluor™ Green 620 Antibody Labeling Kit *Microscale Optimized for Labeling 50 µg Antibody Per Reaction* | 2 Labelings | 1123 |
| ReadiLink™ Rapid mFluor™ Yellow 630 Antibody Labeling Kit *Microscale Optimized for Labeling 50 µg Antibody Per Reaction* | 2 Labelings | 1126 |
| ReadiLink™ Rapid mFluor™ Red 700 Antibody Labeling Kit *Microscale Optimized for Labeling 50 µg Antibody Per Reaction* | 2 Labelings | 1130 |
| ReadiLink™ Rapid mFluor™ Red 780 Antibody Labeling Kit *Microscale Optimized for Labeling 50 µg Antibody Per Reaction* | 2 Labelings | 1131 |
| mFluor™ UV375 SE | 1 mg | 1135 |
| mFluor™ UV460 SE | 1 mg | 1136 |

| Product | Unit Size | Cat No. |
|---|---|---|
| mFluor™ Violet 500 SE | 1 mg | 1149 |
| mFluor™ Violet 450 SE | 1 mg | 1150 |
| mFluor™ Violet 510 SE | 1 mg | 1151 |
| mFluor™ Violet 540 SE | 1 mg | 1152 |
| mFluor™ Violet 550 SE | 1 mg | 1153 |
| mFluor™ Violet 505 SE | 1 mg | 1154 |
| mFluor™ Violet 590 SE | 1 mg | 1155 |
| mFluor™ Violet 610 SE | 1 mg | 1156 |
| mFluor™ Violet 545 SE | 1 mg | 1157 |
| mFluor™ Blue 570 SE | 1 mg | 1160 |
| mFluor™ Blue 590 SE | 1 mg | 1161 |
| mFluor™ Blue 620 SE | 1 mg | 1163 |
| mFluor™ Blue 630 SE | 1 mg | 1164 |
| mFluor™ Green 620 SE | 1 mg | 1165 |
| mFluor™ Green 630 SE | 1 mg | 1168 |
| mFluor™ Yellow 630 SE | 1 mg | 1170 |
| mFluor™ Blue 580 SE | 1 mg | 1178 |
| mFluor™ Blue 660 SE | 1 mg | 1180 |
| mFluor™ Red 700 SE | 1 mg | 1190 |
| mFluor™ Red 780 SE | 1 mg | 1191 |
| Buccutite™ Rapid PE Antibody Labeling Kit *Microscale Optimized for Labeling 100 ug Antibody Per Reaction* | 2 Labelings | 1310 |
| Buccutite™ Rapid APC Antibody Labeling Kit *Microscale Optimized for Labeling 100 ug Antibody Per Reaction* | 2 Labelings | 1311 |
| Buccutite™ Rapid PE Antibody Labeling Kit *Microscale Optimized for Labeling 25 ug Antibody Per Reaction* | 2 Labelings | 1312 |
| Buccutite™ Rapid APC Antibody Labeling Kit *Microscale Optimized for Labeling 25 ug Antibody Per Reaction* | 2 Labelings | 1313 |
| Buccutite™ Rapid PE-Cy5.5 Tandem Antibody Labeling Kit *Microscale Optimized for Labeling 100 ug Antibody Per Reaction* | 2 Labelings | 1316 |
| Buccutite™ Rapid PE-Cy7 Tandem Antibody Labeling Kit *Microscale Optimized for Labeling 100 ug Antibody Per Reaction* | 2 Labelings | 1317 |
| Buccutite™ Rapid PE-Texas Red Tandem Antibody Labeling Kit *Microscale Optimized for Labeling 100 ug Antibody Per Reaction* | 2 Labelings | 1318 |
| Buccutite™ Rapid APC-iFluor™ 700 Tandem Antibody Labeling Kit *Microscale Optimized for Labeling 100 ug Antibody Per Reaction* | 2 Labelings | 1319 |
| Buccutite™ Rapid APC-Cy5.5 Tandem Antibody Labeling Kit *Microscale Optimized for Labeling 100 ug Antibody Per Reaction* | 2 Lalelings | 1320 |
| Buccutite™ Rapid APC-Cy7 Tandem Antibody Labeling Kit *Microscale Optimized for Labeling 100 ug Antibody Per Reaction* | 2 Labelings | 1321 |
| Buccutite™ Rapid PE-Cy5 Tandem Antibody Labeling Kit *Microscale Optimized for Labeling 100 ug Antibody Per Reaction* | 2 Labelings | 1322 |
| Buccutite™ Rapid PE-Cy5 Tandem Antibody Labeling Kit *Microscale Optimized for Labeling 25 ug Antibody Per Reaction* | 2 Labelings | 1340 |
| Buccutite™ Rapid PE-Cy5.5 Tandem Antibody Labeling Kit *Microscale Optimized for Labeling 25 ug Antibody Per Reaction* | 2 Labelings | 1341 |
| Buccutite™ Rapid PE-Cy7 Tandem Antibody Labeling Kit *Microscale Optimized for Labeling 25 ug Antibody Per Reaction* | 2 Labelings | 1342 |

| Product | Unit Size | Cat No. |
|---|---|---|
| Buccutite™ Rapid PE-Texas Red Tandem Antibody Labeling Kit *Microscale Optimized for Labeling 25 ug Antibody Per Reaction* | 2 Labelings | 1343 |
| Buccutite™ Rapid APC-iFluor™ 700 Tandem Antibody Labeling Kit *Microscale Optimized for Labeling 25 ug Antibody Per Reaction* | 2 Labelings | 1347 |
| Buccutite™ Rapid APC-Cy5.5 Tandem Antibody Labeling Kit *Microscale Optimized for Labeling 25 ug Antibody Per Reaction* | 2 Labelings | 1350 |
| Buccutite™ Rapid APC-Cy7 Tandem Antibody Labeling Kit *Microscale Optimized for Labeling 25 ug Antibody Per Reaction* | 2 Labelings | 1351 |
| mFluor™ UV420 SE | 1 mg | 1641 |
| mFluor™ UV455 SE | 1 mg | 1642 |
| mFluor™ UV520 SE | 1 mg | 1643 |
| mFluor™ UV540 SE | 1 mg | 1645 |
| mFluor™ UV610 SE | 1 mg | 1649 |
| ReadiUse™ PE [R-Phycoerythrin] *Ammonium Sulfate-Free* | 1 mg | 2500 |
| ReadiUse™ PE [R-Phycoerythrin] *Ammonium Sulfate-Free* | 10 mg | 2501 |
| ReadiUse™ CL-APC [Cross linked-Allophycocyanin] *Ammonium Sulfate-Free* | 1 mg | 2503 |
| ReadiUse™ CL-APC [Cross linked-Allophycocyanin] *Ammonium Sulfate-Free* | 10 mg | 2504 |
| CL-APC [Cross linked-AlloPhycocyanin] | 10 mg | 2549 |
| CL-APC [Cross linked-AlloPhycocyanin] | 50 mg | 2550 |
| CL-APC [Cross linked-AlloPhycocyanin] | 100 mg | 2551 |
| CL-APC [Cross linked-AlloPhycocyanin] | 1 mg | 2552 |
| APC [Allophycocyanin] | 1 mg | 2554 |
| APC [Allophycocyanin] | 10 mg | 2555 |
| PE [R-Phycoerythrin] *CAS 11016-17-4* | 10 mg | 2556 |
| PE [R-Phycoerythrin] *CAS 11016-17-4* | 100 mg | 2557 |
| PE [R-Phycoerythrin] *CAS 11016-17-4* | 1 mg | 2558 |
| ReadiUse™ Preactivated APC | 1 mg | 2561 |
| ReadiUse™ Preactivated APC-iFluor™ 700 Tandem | 1 mg | 2570 |
| ReadiUse™ Preactivated APC-iFluor™ 750 Tandem | 1 mg | 2571 |
| ReadiUse™ Preactivated APC-iFluor™ 800 Tandem | 1 mg | 2572 |
| ReadiUse™ Preactivated PE-iFluor™ 647 Tandem | 1 mg | 2577 |
| ReadiUse™ Preactivated PE-iFluor™ 750 Tandem | 1 mg | 2578 |
| ReadiUse™ Preactivated PE-iFluor™ 660 Tandem | 1 mg | 2579 |
| ReadiUse™ Preactivated PE-Cy5 Tandem | 1 mg | 2580 |
| ReadiUse™ Preactivated PE-Cy5.5 Tandem | 1 mg | 2581 |
| ReadiUse™ Preactivated PE-Cy7 Tandem | 1 mg | 2582 |
| ReadiUse™ Preactivated PE-Texas Red Tandem | 1 mg | 2583 |
| ReadiUse™ Preactivated PE-iFluor™ 594 Tandem | 1 mg | 2584 |

| Product | Unit Size | Cat No. |
|---|---|---|
| ReadiUse™ Preactivated PE-iFluor™ 700 Tandem | 1 mg | 2585 |
| ReadiUse™ Preactivated APC-Cy5.5 Tandem | 1 mg | 2586 |
| ReadiUse™ Preactivated APC-Cy7 Tandem | 1 mg | 2587 |
| PE-iFluor™ 594 Tandem | 1 mg | 2600 |
| PE-iFluor™ 660 Tandem | 1 mg | 2602 |
| PE-Cy5 Tandem | 1 mg | 2610 |
| PE-Cy5.5 Tandem | 1 mg | 2613 |
| PE-iFluor™ 700 Tandem | 1 mg | 2614 |
| PE-iFluor™ 710 Tandem | 1 mg | 2615 |
| PE-Cy7 Tandem | 1 mg | 2616 |
| PE-Texas Red Tandem | 1 mg | 2619 |
| APC-Cy5.5 Tandem | 1 mg | 2622 |
| APC-iFluor™ 700 Tandem | 1 mg | 2623 |
| APC-XFD700 Tandem | 1 mg | 2624 |
| APC-Cy7 Tandem | 1 mg | 2625 |
| APC-iFluor™ 750 Tandem | 1 mg | 2626 |
| APC-XFD750 Tandem | 1 mg | 2627 |
| APC-iFluor™ 800 Tandem | 1 mg | 2630 |
| PE-iFluor™ 610 Tandem | 1 mg | 2700 |
| PE-iFluor™ 647 Tandem | 1 mg | 2702 |
| PE-iFluor™ 750 Tandem | 1 mg | 2704 |
| Purified Anti-human CD1 Antibody *HI149* | 100 ug | 10010000 |
| Purified Anti-human CD1 Antibody *OKT-6* | 100 ug | 10011000 |
| Purified Anti-human CD1 Antibody *SN13* | 100 ug | 10012000 |
| Purified Anti-human CD1 Antibody *L161* | 100 ug | 10013000 |
| Purified Anti-human CD3 Antibody *HIT3a* | 100 ug | 10030000 |
| Purified Anti-human CD3 Antibody *HIT3b* | 100 ug | 10031000 |
| Purified Anti-human CD3 Antibody *UCHT1* | 100 ug | 10032000 |
| Purified Anti-human CD3 Antibody *SK7* | 100 ug | 10033000 |
| Purified Anti-human CD3 Antibody *OKT-3* | 100 ug | 10034000 |
| Purified Anti-human CD4 Antibody *HIT4a* | 100 ug | 10040000 |
| Purified Anti-human CD4 Antibody *RPA-T4* | 100 ug | 10041000 |
| Purified Anti-human CD4 Antibody *SK3* | 100 ug | 10042000 |
| Purified Anti-human CD4 Antibody *OKT-4* | 100 ug | 10043000 |

| Product | Unit Size | Cat No. |
|---|---|---|
| Purified Anti-human CD8 Antibody *HIT8a* | 100 ug | 10080000 |
| Purified Anti-human CD8 Antibody *SK1* | 100 ug | 10081000 |
| Purified Anti-human CD8 Antibody *OKT-8* | 100 ug | 10082000 |
| Purified Anti-human CD11b Antibody *HI11b* | 100 ug | 10111000 |
| Purified Anti-human CD11b Antibody *ICRF44* | 100 ug | 10112000 |
| Purified Anti-human CD11c Antibody *3.9* | 100 ug | 10113000 |
| Purified Anti-human CD14 Antibody *61D3* | 100 ug | 10141000 |
| Purified Anti-human CD16 Antibody *HI16a* | 100 ug | 10160000 |
| Purified Anti-human CD16 Antibody *3G8* | 100 ug | 10161000 |
| Purified Anti-human CD19 Antibody *HI19a* | 100 ug | 10190000 |
| Purified Anti-human CD19 Antibody *SJ25C1* | 100 ug | 10191000 |
| Purified Anti-human CD19 Antibody *HIB19* | 100 ug | 10192000 |
| Purified Anti-human CD19 Antibody *4G7* | 100 ug | 10193000 |
| Purified Anti-human CD25 Antibody *HI25a* | 100 ug | 10250000 |
| Purified Anti-human CD25 Antibody *7G7B6* | 100 ug | 10251000 |
| Purified Anti-human CD27 Antibody *LT27* | 100 ug | 10270000 |
| Purified Anti-human CD27 Antibody *O323* | 100 ug | 10271000 |
| Purified Anti-human CD28 Antibody *CD28.2* | 100 ug | 10280000 |
| Purified Anti-human CD28 Antibody *9.3* | 100 ug | 10281000 |
| Purified Anti-human CD38 Antibody *HIT2* | 100 ug | 10380000 |
| Purified Anti-human CD38 Antibody *HI157* | 100 ug | 10381000 |
| Purified Anti-human CD38 Antibody *HB7* | 100 ug | 10382000 |
| Purified Anti-human CD45 Antibody *HI30* | 100 ug | 10450000 |
| Purified Anti-human CD45 Antibody *HI73* | 100 ug | 10451000 |
| Purified Anti-human CD45 Antibody *HI185* | 100 ug | 10453000 |
| Purified Anti-human CD45 Antibody *2D1* | 100 ug | 10454000 |
| Purified Anti-human CD45 Antibody *HI100* | 100 ug | 10455000 |
| Purified Anti-human CD45 Antibody *UCHL1* | 100 ug | 10456000 |
| Purified Anti-human CD56 Antibody *B-A19* | 100 ug | 10560000 |
| Purified Anti-human CD56 Antibody *My31* | 100 ug | 10562000 |
| Purified Anti-human CD57 Antibody *HI57a* | 100 ug | 10570000 |
| Purified Anti-human CD95 Antibody *EOS9.1* | 100 ug | 10950000 |
| Purified Anti-human CD123 Antibody *12H7* | 100 ug | 11231000 |
| Purified Anti-human CD3 Antibody *HIT3b* | 100 ug | 10031000 |

# Frontiers in Serodiagnostics

## A New Plasmon-Enhanced Fluorescence Biosensor Technology Suitable for Lab-on-a-Chip Applications


### *Abstract*

*Host response to microbes may be detected in human serum using a variety of plasmonic-based technology platforms, including localized surface plasmon resonance, propagating surface plasma resonance, surface-enhanced Raman scattering, surface-enhanced infrared absorption spectroscopy, and various surface-enhanced fluorescence methods. One recently devised adaptation of Grating-Coupled Surface Plasmon Resonance (GC-SPR) is referred to as Grating-Coupled Fluorescent Plasmonics (GC-FP). The feasibility of using this new technology for detecting immune responses to microbes has only recently been demonstrated in the context of Lyme disease and Covid-19 infections. While still in a relatively early stage of technology development, this GC-SPR-based method holds promise in democratizing lab-on-a-chip serologic testing for widespread deployment in point-of-care (POC) diagnostic environments.*


## Introduction

Standard microbial detection approaches typically demand relatively expensive assay kits, sophisticated instrumentation, and expert handling, as exemplified by gene sequencing, polymerase chain reaction (PCR), hemagglutination assay, Western blotting (WB), lateral flow immunoassay (LFIA), and enzyme-linked immunosorbent assay (ELISA). Additionally, the pre-developed protocols for particular pathogens are usually limited to specific strains or types of microbes. Conventional techniques such as ELISA and LFIA often provide sufficient sensitivity to detect individual analytes at physiologic concentrations. However, the cost per analyte scales linearly and becomes impractical when evaluating complex multi-analyte systems. WB allows simultaneous measurement of multiple antibodies but is limited by sensitivity, specificity, resolution of the electrophoretic separation medium, and assay complexity. Increasingly there is a need for higher content, more sensitive, more specific, less expensive, and easier-to-use alternatives to ELISA, LFIA, and WB for antigen detection. Plasmonic-based biosensing technologies may potentially provide such an alternative approach to microbial antigen detection, offering highly sensitive and rapid diagnosis, with minimal sample pretreatment, easy operation, and inexpensive instrumentation (Niu et al., 2015; Shrivastav et al., 2021).

## GC-SPR and GC-FP Technology

Surface plasmon resonance (SPR)-based immunosensors provide a nondestructive optical analysis approach which is useful for examining antigen-antibody interactions for biomolecules deposited in a thin layer on the surface of a gold-coated sensor chip (Rossi et al., 2018). Many optical biosensors utilize the principle of SPR, the resonant oscillation of conduction electrons at the interface between negative and positive permittivity material stimulated by incident light. The surface plasmon polariton (SPP) is a non-radiative electromagnetic surface wave that propagates in a direction parallel to the negative permittivity/dielectric material interface. Since the wave is localized at the boundary of the conductor and the external medium (e.g., air, buffer, or serum), these oscillations are particularly sensitive to any perturbation of this boundary,

such as can occur through the adsorption of macromolecules to the conducting surface. Standard SPR-based sensors offer the advantage of being label-free, enzyme-free, real-time, and readily implemented in cost-effective integrated devices.

Surface plasmon resonance (SPR)-based immunosensors provide a nondestructive optical analysis approach which is useful for examining antigen-antibody interactions for biomolecules deposited in a thin layer on the surface of a gold-coated sensor chip (Rossi et al., 2018). Many optical biosensors utilize the principle of SPR, the resonant oscillation of conduction electrons at the interface between negative and positive permittivity material stimulated by incident light. The surface plasmon polariton (SPP) is a non-radiative electromagnetic surface wave that propagates in a direction parallel to the negative permittivity/dielectric material interface. Since the wave is localized at the boundary of the conductor and the external medium (e.g., air, buffer, or serum), these oscillations are particularly sensitive to any perturbation of this boundary, such as can occur through the adsorption of macromolecules to the conducting surface. Standard SPR-based sensors offer the advantage of being label-free, enzyme-free, real-time, and readily implemented in cost-effective integrated devices.

One widely used approach to deliver coupling between incident light and SPP for SPR sensing of biological macromolecules is through the use of a prism. Unfortunately, however, the awkward and complex optical system required for prism-based devices often limits its versatility and ease of integration into miniaturized arrays for lab-on-a-chip applications. In contrast to prism-based SPR, for grating-based coupling devices (GC-SPR), resonance conditions are provided by diffraction of the incident light, offering greater opportunity for miniaturization and integration into lab-on-a-chip platforms (Figure 1). However, one drawback to grating-based relative to prism-based systems is their overall poorer detection sensitivity and consequently poorer target limit of detection (LOD).

In GC-FP, the interaction of fluorophores with surface plasmons amplifies fluorescence signal (brightness) accompanying molecular binding events by several orders of

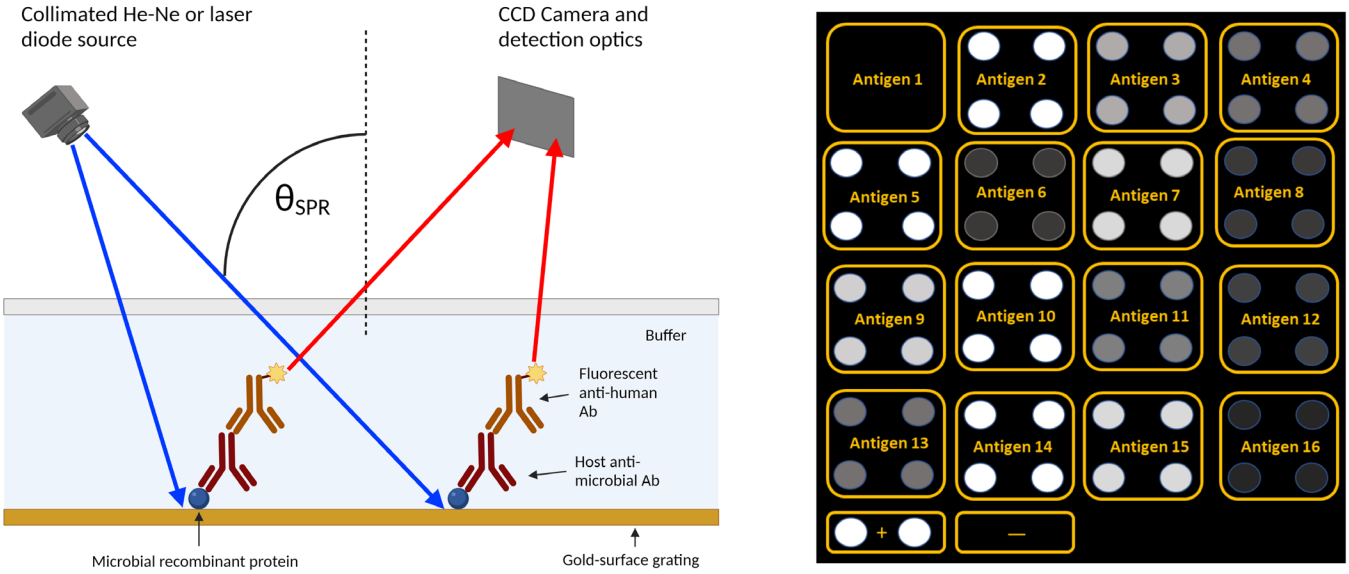


**Figure 1.** The development of microscopic sensing platforms combined with microfluidics has facilitated integrating sensors and microarrays into lab-on-a-chip devices. A schematic diagram of GC-FP analysis on a gold-coated GC-SPR chip is shown (left), using fluorophore-conjugated antibodies to enhance the signal. In the example shown, an array of recombinant proteins (68 total features) is exposed to blood serum from an infected patient. Antibodies present in the serum bind to a subset of protein antigens displayed on the array and are subsequently highlighted by addition of a fluorophore-labeled secondary antibody, such as goat anti-mouse (GAM) secondary antibody, leading to a shift in the SPR signal. A representative GC-FP image (right) is schematically depicted, providing a characteristic "constellation" of bright spots due to antibody binding to a subset of target proteins, which indicates exposure to the microbial disease. Recombinant microbial proteins are depicted as antigens 1-16 in the diagram. – and + represent negative and positive control spots, respectively. In the example shown, host antibodies reacted strongly with microbial antigens 2, 5, 7, 10, 14 and 15.

magnitude. GC-FP technology enables multiplexed biomarker screening of blood serum using a GC-SPR microchip that can be imaged with a complementary metal-oxide-semiconductor (CMOS) or charge-coupled device (CCD) camera and subsequently algorithmically scored to aid in achieving a diagnosis. The SPR effect can enhance the reporter signal by 2-3 orders of magnitude and can aid in quantifying a variety of biological attributes, such as a heterogeneous population of antibodies within the sample, using an intuitive microarray format.

## Applications: COVID-19 and Lyme Disease Serodiagnostics

Several key biomedical indications demand sensitive antibody-based testing in the clinical setting, including characterization of individual immune response arising from vaccination and the assessment of herd immunity in population-based health studies, as exemplified by the recent COVID-19 pandemic, as well as the diagnosis of infections arising from low-titer organisms, as exemplified by Lyme disease. It is becoming increasingly apparent that most clinically relevant disease states can be better characterized by tracking panels of biomarkers, as a particular clinical phenotype may be definable by hundreds of changes at the molecular and cellular level. The feasibility of detecting panels of biomarkers in COVID-19 and Lyme disease using GC-FP has recently been demonstrated, as described below.

### COVID-19

Recently, humanity has been attempting to deal with the public health emergency of the 2019 SARS CoV-2 (COVID-19) pandemic, which is believed to have originated from Wuhan, China, in December 2019, before rapidly spreading across the globe (Pascarella et al., 2020). The disease is characterized by flu-like symptoms, which can become especially life-threatening in high-risk individuals. Specifically, symptoms include conjunctivitis, cough, fatigue, fever, gastrointestinal disturbances, headache, labored breathing, loss of taste, loss of smell, and sore throat. As of August 2021, more than 200 million people have contracted the disease worldwide, with a global death toll of roughly 4.5 million. COVID-19 is transmitted from human to human through the air in respiratory droplets and upon physical contact with contaminated environmental surfaces. In order to minimize loss of life from this new pandemic and to increase preparedness for any future reemergence of COVID-19 variants, as well as other future pandemics, rapid and timely diagnostic assays are urgently required (Pascarella et al., 2020).

Plasmonic-based biosensor assays potentially offer advantages with respect to viral diagnostics, including low assay cost, low instrument cost, fast implementation, and ease of use. GC-FP has recently been employed to monitor antibody-antigen binding interactions for multiple targets in individual COVID-19 patient serum samples (Cady et al., 2021; Cognetti et al., 2021). Recombinant nucleocapsid protein, the S1 fragment of the spike protein, the extracellular domain of the spike protein, the receptor-binding domain of the spike protein, the S1 domain of the 2005 SARS coronavirus spike protein, and human Influenza B nucleoprotein IgG were spotted in replicates of three onto gold-coated silicon microchips containing a plasmonic diffraction grating, using a robotic spotter. Human serum albumin (HSA) and human IgG were included on the microarrays as negative and positive spotting controls, respectively. Microarrays were blocked to minimize nonspecific binding, then incubated with diluted serum sample, followed by far-red emitting fluorophore-labeled IgG/IgM antibodies, with washes after the serum and antibody incubations. Microarrays were analyzed using a GC-SPR instrument developed by Ciencia, Inc. (East Hartford, CT), equipped with an incident collimated 633 nm laser beam.

Initial results established 100% selectivity and sensitivity (n = 23) in detecting serum IgG levels raised against three common COVID-19 antigens, spike S1, spike S1S2, and the nucleocapsid protein. The assay was revealed to provide quantitative data across serum dilutions ranging from 1:25–1:1,600. This feasibility study also demonstrated a strong correlation of results with commercially available ELISA and Luminex-based immunoassays, though ELISA provided a superior LOD. The time required to perform antibody detection by GC-FP was determined to be roughly 30 minutes, which is significantly

shorter than the standard 2-3 hours required to complete ELISA or Luminex-based assays. The investigators demonstrated the feasibility of detecting COVID-19 from dried blood spots, reducing the complexity of sample collection, handling, transport, and storage relative to standard venipuncture-based whole blood collection.

## Lyme Disease

Lyme disease afflicts 300,000 - 450,000 people annually, primarily in the Great Lakes and Northeastern regions of the United States and portions of Canada. The disease is primarily caused by the bacterium Borrelia burgdorferi, though rarely it can also be spread by Borrelia mayonii (Moore et al., 2016). It is transmitted to humans through the bite of infected black-legged ticks (Figure 2), which also infect deer populations in the cited regions. Common symptoms arising from infection include headache, fever, fatigue, and a characteristic skin rash. If the disease is not treated, the infection can ultimately spread to joints (arthritis), the heart (carditis, heart arrhythmia), and the nervous system (meningitis, neuropathy). Lyme disease is generally diagnosed based upon patient symptoms, the presence of a characteristic rash (erythema migrans), and the likelihood of exposure to infected ticks in the environment. Laboratory testing using validated antigen assays, as briefly described below, is required to confirm the presence of the disease. In most instances, Lyme disease can be successfully treated using a regime of antibiotics over the course of several weeks.

The U.S. Center for Disease Control (CDC) recommends a standard two-tiered test (STTT) for diagnosing Lyme disease. The first tier employs either ELISA or an immunofluorescence assay, while the second tier is WB. However, the STTT used to diagnose Lyme disease displays relatively poor sensitivity, especially during the early stages of disease progression, often reporting false-negative results. Conversely, false-positive test results may occur from circulating antibodies remaining in the patient's system for years' post-infection and after resolution of the infection.

A protein microarray has recently been fabricated to measure potentially diagnostic host serum antibody targets to Lyme disease using GC-FP technology (Chou et al., 2020; 2021). Recombinant Borrelia burgdorferi proteins (BmpA, OspD, OspC, DbpA, DbpB, RevA, ErpG, ErpL, ErpY, VlsE, BBA65, BBA69, BBA70, BBA73, P41, and p48) were spotted in replicates of four onto gold-coated silicon microchips containing a plasmonic diffraction grating, using a robotic spotter. Bovine serum albumin (BSA) and human IgG were included on the microarrays as negative and positive spotting controls, respectively. Microarrays were blocked to minimize nonspecific binding, then incubated with diluted serum sample, followed by far-red emitting fluorophore-labeled IgG and IgM antibodies, with washes after the serum and each antibody incubation. Microarrays were analyzed using a GC-SPR instrument developed by Ciencia, Inc, equipped with an incident collimated 633 nm laser beam.

**Figure 2.** The black legged tick is a common arthropod vector that transmits Lyme disease to humans. Most humans are infected through the bites of immature ticks called nymphs, feeding during the spring and summer months. Since ticks don't fly or jump, they wait for hosts while resting on the tips of grasses and shrubs. When a host brushes up against the plant, the tick hastily climbs aboard and then finds a suitable place to bite the host, usually in difficult-to-see regions of the body, such as the armpits, groin, or scalp.

The cited analytical approach requires low microliter volumes of human serum to facilitate multiplexed biomarker screening of femtomole levels of host antibodies using a compact microarray surface. The approach produces semi-quantitative results (~6-fold linear dynamic range, Chou et al., 2020) that can be further processed to obtain a diagnostic score. The semi-quantitative, high-sensitivity nature of GC-FP enabled the screening of antibody targets for predictive value in determining Lyme disease status and the creation of a diagnostic algorithm that was more sensitive, specific, and informative than standard ELISA and WB assays. The diagnostic algorithm appeared to be more sensitive than the current CDC STTT standard for detecting early Lyme disease while maintaining 100% specificity. Furthermore, analysis of relative IgG and IgM serum antibody levels to predict disease status, such as acute-versus-convalescent stages of infection,

appears feasible using GC-FP.

## Fluorescent Conjugates

Biosensors are typically comprised of three main components: the target, recognition, and transducing portions. The target is the analyte of interest, which is detected when it is captured by the recognition element through some specific interaction. Upon binding to the target molecule, the recognition element of the sensor undergoes a change in one of its physical or chemical properties, such as conductivity, refractive index (RI), absorbance maxima, or pH value. This property change is translated to a readable signal with the aid of a transducer.

The selection of suitable fluorophore conjugates depends upon a particular instrument's design and set-up. The cited platforms for microbial host response detection described in this review rely upon a Helium-Neon or laser diode light source. In order to separate incident light at the excitation wavelength from the SPP-stimulated fluorescence emission signal, a set of

**Table 1.** Suitable fluorophore conjugates for detecting host-generated microbial antibodies based upon fluorescence emission excitation by grating-coupled SPPs. Reactive versions of the fluorophores are also available to facilitate custom labeling of specific biological targets.

| Recommended fluorophore conjugates for Helium-Neon laser (632.8 nm) or laser diode (637 nm) sources | Abs max (nm) | Em max (nm) | Catalog Number (200 µg) |
|---|---|---|---|
| iFluor™ 633 Goat Anti-human IgG (H+L) Antibody | 638 | 652 | 50092 |
| iFluor™ 633 Goat Anti-human IgG (H+L) Antibody *Cross Adsorbed* | 638 | 652 | 50094 |
| APC Goat Anti-human IgG (H+L) Antibody | 651 | 660 | 50184 |
| APC Goat Anti-human IgG (H+L) Antibody *Cross Adsorbed* | 651 | 660 | 50186 |
| PE/Cy5 Goat Anti-human IgG (H+L) Antibody | 565 | 666 | 50224 |
| PE/Cy5 Goat Anti-human IgG (H+L) Antibody *Cross Adsorbed* | 565 | 666 | 50226 |
| PE/iFluor™ 647 Goat Anti-human IgG (H+L) Antibody | 569 | 666 | 50240 |
| PE/iFluor™ 647 Goat Anti-human IgG (H+L) Antibody *Cross Adsorbed* | 569 | 666 | 50242 |
| iFluor™ 647 Goat Anti-human IgG (H+L) Antibody | 654 | 669 | 50096 |
| iFluor™ 647 Goat Anti-human IgG (H+L) Antibody *Cross Adsorbed* | 654 | 669 | 50098 |
| XFD647 Goat Anti-human IgG (H+L) Antibody | 650 | 671 | 50168 |
| XFD647 Goat Anti-human IgG (H+L) Antibody *Cross Adsorbed, | 650 | 671 | 50170 |
| iFluor™ 660 Goat Anti-human IgG (H+L) Antibody | 663 | 678 | 50100 |
| iFluor™ 660 Goat Anti-human IgG (H+L) Antibody *Cross Adsorbed* | 663 | 678 | 50102 |
| iFluor™ 670 Goat Anti-human IgG (H+L) Antibody | 671 | 682 | 50104 |
| iFluor™ 670 Goat Anti-human IgG (H+L) Antibody *Cross Adsorbed* | 671 | 682 | 50106 |
| iFluor™ 680 Goat Anti-human IgG (H+L) Antibody | 684 | 701 | 50108 |
| iFluor™ 680 Goat Anti-human IgG (H+L) Antibody *Cross Adsorbed* | 684 | 701 | 50110 |
| iFluor™ 700 Goat Anti-human IgG (H+L) Antibody | 690 | 713 | 50112 |
| iFluor™ 700 Goat Anti-human IgG (H+L) Antibody *Cross Adsorbed* | 690 | 713 | 50114 |
| PE/AF 700 Goat Anti-human IgG (H+L) Antibody | 566 | 721 | 50236 |
| PE/AF 700 Goat Anti-human IgG (H+L) Antibody *Cross Adsorbed* | 566 | 721 | 50238 |
| iFluor™ 710 Goat Anti-human IgG (H+L) Antibody | 717 | 739 | 50116 |
| iFluor™ 710 Goat Anti-human IgG (H+L) Antibody *Cross Adsorbed* | 717 | 739 | 50118 |
| APC/iFluor™ 700 Goat Anti-human IgG (H+L) Antibody | 650 | 775 | 50196 |
| APC/iFluor™ 700 Goat Anti-human IgG (H+L) Antibody *Cross Adsorbed* | 650 | 775 | 50198 |
| PE/Cy7 Goat Anti-human IgG (H+L) Antibody | 566 | 778 | 50228 |
| PE/Cy7 Goat Anti-human IgG (H+L) Antibody *Cross Adsorbed* | 566 | 778 | 50230 |
| PE/iFluor™ 750 Goat Anti-human IgG (H+L) Antibody | 566 | 778 | 50244 |
| PE/iFluor™ 750 Goat Anti-human IgG (H+L) Antibody *Cross Adsorbed* | 566 | 778 | 50246 |
| APC/Cy7 Goat Anti-human IgG (H+L) Antibody | 651 | 779 | 50188 |
| APC/Cy7 Goat Anti-human IgG (H+L) Antibody *Cross Adsorbed* | 651 | 779 | 50190 |
| APC/XFD750 Goat Anti-human IgG (H+L) Antibody | 650 | 785 | 50192 |
| APC/XFD750 Goat Anti-human IgG (H+L) Antibody *Cross Adsorbed* | 650 | 785 | 50194 |
| APC/iFluor™ 750 Goat Anti-human IgG (H+L) Antibody | 650 | 790 | 50200 |
| APC/iFluor™ 750 Goat Anti-human IgG (H+L) Antibody *Cross Adsorbed* | 650 | 790 | 50202 |

bandpass filters is typically employed. For He-Ne and laser diode laser sources, the selected bandpass filters have typically been centered at about 670 nm, matching the emission maximum of the Alexa Fluor® 647 fluorophore (Note: AAT Bioquest's XFD647 fluorophore has an identical structure as Alexa Fluor® 647 dye). However, conceivably longer wavelength bandpass filters could be employed for fluorophores emitting further in the red region of the spectrum. AAT Bioquest offers more than 100 different fluorescent, biotinylated, and enzyme-labeled goat anti-human secondary antibodies that are potentially suitable for GC-FP biosensor technology. The compendium of fluorophore conjugates that could potentially be utilized for GC-FP using commercially available instrumentation is summarized in Table 1.

## Conclusion

A wide range of conventional viral sensors have been devised over the years, often for biomedical and agricultural applications, which have been based upon chromatography, mass-sensitive, or electrochemical (amperometric, potentiometric, impedimetric, and calorimetric) signal transduction approaches (Bauch et al., 2014; Shrivastav et al., 2021). Plasmonics-based sensors offer several advantages compared to these conventional approaches, including real-time monitoring to probe the binding dynamics involved in various biomolecular interactions, short response time, device reusability, and simple sample preparation, as well as the use of relatively few electrical components in the detection platform, which is conducive to assay miniaturization. Limitations encountered with the class of biosensors include the nonspecific nature of the binding surface, which can be somewhat abrogated by immobilizing an analyte selective layer over the plasmonic film, mass transportation limitations, and steric hindrance during the target binding event. GC-FP is a relatively new SPR-based detection technology currently being benchmarked in R&D laboratories. Only time will tell whether this technology successfully runs the gauntlet of regulatory tests necessary for its full authorization as a POC lab–on–a–chip diagnostic platform.

## References


1. Bauch, M., Toma, K., Toma, M., Zhang, Q, Dostalek, J. (2014) "Plasmon-Enhanced Fluorescence Biosensors: a Review." Plasmonics 9, 781–799.
2. Cady, N. C., Tokranova, Minor, N.A., Nikvand, N., Strle, K., Lee, W.T., Page, W., Guignon, Pilar, E.A., Gibson, G.N. (2021) "Multiplexed detection and quantification of human antibody response to COVID-19 infection using a plasmon enhanced biosensor platform." Biosensors and Bioelectronics,171, 112679.
3. Chou E, Lasek-Nesselquist E, Taubner B, Pilar A, Guignon E, Page W, Lin, Y.P., Cady, N.C. (2020) "A fluorescent plasmonic biochip assay for multiplex screening of diagnostic serum antibody targets in human Lyme disease." PLoS ONE 15(2): e0228772.
4. Chou E, Minor A, Cady NC. (2021) "Quantitative multiplexed strategies for human Lyme disease serological testing." Exp Biol Med (Maywood);246(12):1388-1399.
5. Cognetti JS, Steiner DJ, Abedin M, Bryan MR, Shanahan C, Tokranova N, Young E, Klose AM, Zavriyev A, Judy N, Piorek B, Meinhart C, Jakubowicz R, Warren H, Cady NC, Miller BL. (2021) "Disposable photonics for cost-effective clinical bioassays: application to COVID-19 antibody testing." Lab Chip. 21(15):2913-2921.
6. Moore A, Nelson C, Molins C, Mead P, Schriefer M. (2016) "Current Guidelines, Common Clinical Pitfalls, and Future Directions for Laboratory Diagnosis of Lyme Disease, United States." Emerg Infect Dis. 22(7):1169–77.
7. Nicol A, Knoll W. (2018) Characteristics of Fluorescence Emission Excited by Grating-Coupled Surface Plasmons. Plasmonics. 13(6):2337-2343.
8. Niu L, Zhang N, Liu H, Zhou X, Knoll W. (2015) Integrating plasmonic diagnostics and microfluidics. Biomicrofluidics; 9(5):052611.
9. Pascarella, G., Strumia, A., Piliego, C., Bruno, F., Del Buono, R., Costa, F. Scarlata, S., Agrò, F.E. (2020) "COVID-19 diagnosis and management: a comprehensive review." J. Intern. Med. 288 (2), 192–206.
10. Rossi S, Gazzola E, Capaldo P, Borile G, Romanato F. (2018) "Grating-Coupled Surface Plasmon Resonance (GC-SPR) Optimization for Phase-Interrogation Biosensing in a Microfluidic Chamber." Sensors (Basel), 18(5):1621.
11. Shrivastav, A.M., Cvelbar, U. & Abdulhalim, I. (2021) "A comprehensive review on plasmonic-based biosensors used in viral diagnostics." Commun Biol 4, 70.


| Product | Unit Size | Cat No. |
|---|---|---|
| iFluor™ 633 Goat Anti-human IgG (H+L) Antibody | 200 ug | 50092 |
| iFluor™ 633 Goat Anti-human IgG (H+L) Antibody | 1 mg | 50093 |
| iFluor™ 633 Goat Anti-human IgG (H+L) Antibody *Cross Adsorbed* | 200 ug | 50094 |
| iFluor™ 633 Goat Anti-human IgG (H+L) Antibody *Cross Adsorbed* | 1 mg | 50095 |

| Product | Unit Size | Cat No. |
|---|---|---|
| iFluor™ 647 Goat Anti-human IgG (H+L) Antibody | 200 ug | 50096 |
| iFluor™ 647 Goat Anti-human IgG (H+L) Antibody | 1 mg | 50097 |
| iFluor™ 647 Goat Anti-human IgG (H+L) Antibody *Cross Adsorbed* | 200 ug | 50098 |
| iFluor™ 647 Goat Anti-human IgG (H+L) Antibody *Cross Adsorbed* | 1 mg | 50099 |
| iFluor™ 660 Goat Anti-human IgG (H+L) Antibody | 200 ug | 50100 |
| iFluor™ 660 Goat Anti-human IgG (H+L) Antibody | 1 mg | 50101 |
| iFluor™ 660 Goat Anti-human IgG (H+L) Antibody *Cross Adsorbed* | 200 ug | 50102 |
| iFluor™ 660 Goat Anti-human IgG (H+L) Antibody *Cross Adsorbed* | 1 mg | 50103 |
| iFluor™ 670 Goat Anti-human IgG (H+L) Antibody | 200 ug | 50104 |
| iFluor™ 670 Goat Anti-human IgG (H+L) Antibody | 1 mg | 50105 |
| iFluor™ 670 Goat Anti-human IgG (H+L) Antibody *Cross Adsorbed* | 200 ug | 50106 |
| iFluor™ 670 Goat Anti-human IgG (H+L) Antibody *Cross Adsorbed* | 1 mg | 50107 |
| iFluor™ 680 Goat Anti-human IgG (H+L) Antibody | 200 ug | 50108 |
| iFluor™ 680 Goat Anti-human IgG (H+L) Antibody | 1 mg | 50109 |
| iFluor™ 680 Goat Anti-human IgG (H+L) Antibody *Cross Adsorbed* | 200 ug | 50110 |
| iFluor™ 680 Goat Anti-human IgG (H+L) Antibody *Cross Adsorbed* | 1 mg | 50111 |
| iFluor™ 700 Goat Anti-human IgG (H+L) Antibody | 200 ug | 50112 |
| iFluor™ 700 Goat Anti-human IgG (H+L) Antibody | 1 mg | 50113 |
| iFluor™ 700 Goat Anti-human IgG (H+L) Antibody *Cross Adsorbed* | 200 ug | 50114 |
| iFluor™ 700 Goat Anti-human IgG (H+L) Antibody *Cross Adsorbed* | 1 mg | 50115 |
| iFluor™ 710 Goat Anti-human IgG (H+L) Antibody | 200 ug | 50116 |
| iFluor™ 710 Goat Anti-human IgG (H+L) Antibody | 1 mg | 50117 |
| iFluor™ 710 Goat Anti-human IgG (H+L) Antibody *Cross Adsorbed* | 200 ug | 50118 |
| iFluor™ 710 Goat Anti-human IgG (H+L) Antibody *Cross Adsorbed* | 1 mg | 50119 |
| XFD647 Goat Anti-human IgG (H+L) Antibody *XFD647 Same Structure to Alexa Fluor™ 647* | 200 ug | 50168 |
| XFD647 Goat Anti-human IgG (H+L) Antibody *XFD647 Same Structure to Alexa Fluor™ 647* | 1 mg | 50169 |
| XFD647 Goat Anti-human IgG (H+L) Antibody *Cross Adsorbed, XFD647 Same Structure to Alexa Fluor™ 647* | 200 ug | 50170 |
| XFD647 Goat Anti-human IgG (H+L) Antibody *Cross Adsorbed, XFD647 Same Structure to Alexa Fluor™ 647* | 1 mg | 50171 |
| APC Goat Anti-human IgG (H+L) Antibody | 200 ug | 50184 |
| APC Goat Anti-human IgG (H+L) Antibody | 1 mg | 50185 |
| APC Goat Anti-human IgG (H+L) Antibody *Cross Adsorbed* | 200 ug | 50186 |
| APC Goat Anti-human IgG (H+L) Antibody *Cross Adsorbed* | 1 mg | 50187 |
| APC/Cy7 Goat Anti-human IgG (H+L) Antibody | 200 ug | 50188 |
| APC/Cy7 Goat Anti-human IgG (H+L) Antibody | 1 mg | 50189 |

| Product | Unit Size | Cat No. |
|---|---|---|
| APC/Cy7 Goat Anti-human IgG (H+L) Antibody *Cross Adsorbed* | 200 ug | 50190 |
| APC/Cy7 Goat Anti-human IgG (H+L) Antibody *Cross Adsorbed* | 1 mg | 50191 |
| APC/XFD750 Goat Anti-human IgG (H+L) Antibody *XFD750 Same Structure to Alexa Fluor™ 750* | 200 ug | 50192 |
| APC/XFD750 Goat Anti-human IgG (H+L) Antibody *XFD750 Same Structure to Alexa Fluor™ 750* | 1 mg | 50193 |
| APC/XFD750 Goat Anti-human IgG (H+L) Antibody *Cross Adsorbed, XFD750 Same Structure to Alexa Fluor™ 750* | 200 ug | 50194 |
| APC/XFD750 Goat Anti-human IgG (H+L) Antibody *Cross Adsorbed, XFD750 Same Structure to Alexa Fluor™ 750* | 1 mg | 50195 |
| APC/iFluor™ 700 Goat Anti-human IgG (H+L) Antibody | 200 ug | 50196 |
| APC/iFluor™ 700 Goat Anti-human IgG (H+L) Antibody | 1 mg | 50197 |
| APC/iFluor™ 700 Goat Anti-human IgG (H+L) Antibody *Cross Adsorbed* | 200 ug | 50198 |
| APC/iFluor™ 700 Goat Anti-human IgG (H+L) Antibody *Cross Adsorbed* | 1 mg | 50199 |
| APC/iFluor™ 750 Goat Anti-human IgG (H+L) Antibody | 200 ug | 50200 |
| APC/iFluor™ 750 Goat Anti-human IgG (H+L) Antibody | 1 mg | 50201 |
| APC/iFluor™ 750 Goat Anti-human IgG (H+L) Antibody *Cross Adsorbed* | 200 ug | 50202 |
| APC/iFluor™ 750 Goat Anti-human IgG (H+L) Antibody *Cross Adsorbed* | 1 mg | 50203 |
| PE/Cy5 Goat Anti-human IgG (H+L) Antibody | 200 ug | 50224 |
| PE/Cy5 Goat Anti-human IgG (H+L) Antibody | 1 mg | 50225 |
| PE/Cy5 Goat Anti-human IgG (H+L) Antibody *Cross Adsorbed* | 200 ug | 50226 |
| PE/Cy5 Goat Anti-human IgG (H+L) Antibody *Cross Adsorbed* | 1 mg | 50227 |
| PE/Cy7 Goat Anti-human IgG (H+L) Antibody | 200 ug | 50228 |
| PE/Cy7 Goat Anti-human IgG (H+L) Antibody | 1 mg | 50229 |
| PE/Cy7 Goat Anti-human IgG (H+L) Antibody *Cross Adsorbed* | 200 ug | 50230 |
| PE/Cy7 Goat Anti-human IgG (H+L) Antibody *Cross Adsorbed* | 1 mg | 50231 |
| PE/AF 700 Goat Anti-human IgG (H+L) Antibody | 200 ug | 50236 |
| PE/AF 700 Goat Anti-human IgG (H+L) Antibody | 1 mg | 50237 |
| PE/AF 700 Goat Anti-human IgG (H+L) Antibody *Cross Adsorbed* | 200 ug | 50238 |
| PE/AF 700 Goat Anti-human IgG (H+L) Antibody *Cross Adsorbed* | 1 mg | 50239 |
| PE/iFluor™ 647 Goat Anti-human IgG (H+L) Antibody | 200 ug | 50240 |
| PE/iFluor™ 647 Goat Anti-human IgG (H+L) Antibody | 1 mg | 50241 |
| PE/iFluor™ 647 Goat Anti-human IgG (H+L) Antibody *Cross Adsorbed* | 200 ug | 50242 |
| PE/iFluor™ 647 Goat Anti-human IgG (H+L) Antibody *Cross Adsorbed* | 1 mg | 50243 |
| PE/iFluor™ 750 Goat Anti-human IgG (H+L) Antibody | 200 ug | 50244 |
| PE/iFluor™ 750 Goat Anti-human IgG (H+L) Antibody | 1 mg | 50245 |
| PE/iFluor™ 750 Goat Anti-human IgG (H+L) Antibody *Cross Adsorbed* | 200 ug | 50246 |
| PE/iFluor™ 750 Goat Anti-human IgG (H+L) Antibody *Cross Adsorbed* | 1 mg | 50247 |

# Fluorescent Tools

## For Studying Mitochondrial Morphology and Function

### *Introduction*

*Mitochondria are the proverbial 'powerhouse' of eukaryotic cells producing a bulk of their energy supply in the form of adenosine triphosphate (ATP). As dynamic organelles, mitochondria can modify their architecture - sometimes taking up as much as 25% of a cell's volume - to accommodate for the cell's metabolic needs and other cellular processes, including signaling, cellular differentiation, cell cycle maintenance, cell growth, and apoptosis. In immunity, the importance of mitochondrial dynamics is apparent, as many pathogens have evolved mechanisms to modulate host cell mitochondrial remodeling and function to promote their survival. The retrograde signaling initiated by dysfunctional mitochondria can give rise to global changes in gene expression that affects cell morphology and function and initiates the propagation of disease processes. Alterations in mitochondrial morphology and function are good indicators of cell health, and multiplexing mitochondrial morphology reagents with probes that assess function can provide more in-depth information about mitochondrial health. AAT Bioquest has developed a wide range of mitochondrial stains and functional reagents to investigate mitochondria in live- and fixed-cell imaging applications. In this article, we highlight a few of our most-cited probes.*

## Mitochondrial Morphology Tools for Live-Cell Imaging

Mitochondria morphology is complex, dynamic, and highly varied. Through tightly regulated fission, fusion, and mitophagy events, mitochondria can appear in various forms within a cell. From fragmented morphologies of small spheres and short to elongated tubules to a reticulated morphology in which the mitochondrion is a single network of many-branched structures. The number of mitochondria present and their location in a cell can also vary and depends on several variables, including cell or tissue type, developmental stage, metabolic requirement, and overall cell health. For instance, liver hepatocytes, which are involved in metabolism, detoxification, and protein synthesis, have about 1000-2000 mitochondria per cell. Because alterations in mitochondrial function result in dramatic modifications to its

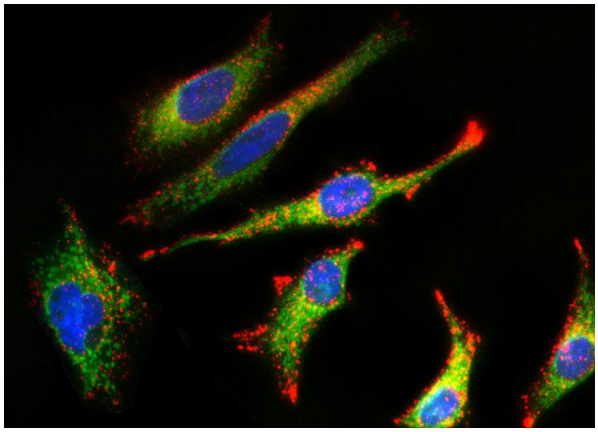

**Figure 1. Co-localization using MitoLite™ Green FM.** Live HeLa cells were incubated with the cell-permeant MitoLite™ Green FM (green) and the red-fluorescent lysosomal stain LysoBrite™ Red (red). Nuclei were counterstained with blue-fluorescent Nuclear Violet™ LCS1.

structure, staining mitochondria using fluorescent dyes such as MitoLite™ dyes and visualizing their morphology through a microscope can provide significant information about their overall biology, localization, and functional state (Table 1). Figure 1 shows HeLa cells with both spheroid-shaped mitochondria and mitochondria with normal reticulated morphology.

## Mitochondrial Functional Tools for Live-Cell Imaging

Mitochondrial dysfunction - characterized by an inadequate number of mitochondria, an inability to provide necessary substrates to mitochondria, or the loss in efficiency of their electron transport chain and reductions in ATP production - is a hallmark of cellular toxicity and is associated with many chronic diseases. These include neurodegenerative disorders, such as Alzheimer's disease and Parkinson's disease, cardiovascular diseases, diabetes, metabolic disorders, autoimmune diseases, gastrointestinal disorders, fatiguing illnesses, musculoskeletal diseases, and chronic infections. AAT Bioquest provides a variety of functional tools for studying mitochondrial function from various perspectives, including probes for mitochondrial membrane potential, autophagy/mitophagy, oxidative phosphorylation, calcium flux, and cytosolic pH (Table 2).

## High-Content Mitochondrial Analysis: Multiplexing Mitochondrial Morphology and Functional Tools

Multiplexing mitochondrial functional tools with morphology probes can significantly improve the study of

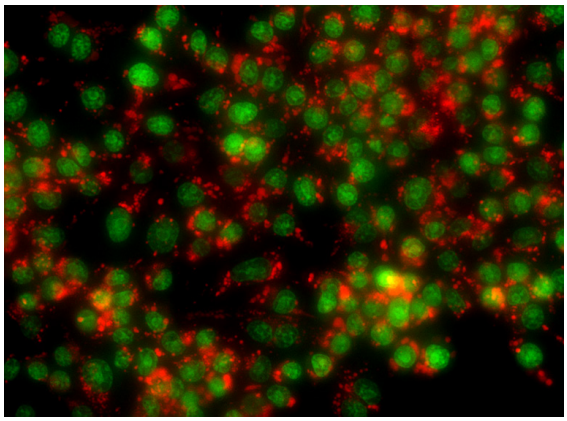

**Figure 2. Mitochondrial hydroxyl radical detection.** RAW 264.7 macrophage cells labeled with Nuclear Green™ LCS1 (green) and hydroxyl radical sensor MitoROS™ OH580 (red) were treated with PMA (phorbol 12-myristate 13-acetate) in a growth medium at 37 °C for four hours to stimulate endogenous hydroxyl radical.

**Table 1.** AAT Bioquest tools for studying mitochondrial morphology.

| Target | Tool | Ex/Em (mn) | Cat No. | Mechanism of action |
|---|---|---|---|---|
| Mitochondria | MitoLite™ Green FM | 508/528 | 22695 | Non-fixable dyes that are sequestered by functioning mitochondria due to the organelle's transmembrane potential. However, cells stained with these dyes will lose their fluorescent staining patterns if mitochondrial function is disrupted or if cells are subjected to fixation and permeabilization. |
| | MitoLite™ Green EX488 | 508/528 | 22675 | |
| | MitoLite™ Orange EX405 | 425/522 | 22679 | |
| | MitoLite™ Blue FX490 | 344/469 | 22674 | Fixable dyes that are sequestered by functioning mitochondria. Cells stained with these dyes retain their fluorescent staining patterns even if mitochondrial function is disrupted or if cells are subjected to fixation and permeabilization. This property makes them useful morphology markers that, once bound, are independent of mitochondrial function. |
| | MitoLite™ Orange FX570 | 553/576 | 22676 | |
| | MitoLite™ Red FX600 | 580/598 | 22677 | |
| | MitoLite™ Red CMXRos | 578/598 | 22698 | |
| | MitoLite™ Deep Red FX660 | 640/659 | 22678 | |
| | MitoLite™ NIR FX690 | 658/691 | 22690 | |
| | CytoFix™ Red Mitochondrial Stain | 510/610 | 23200 | Selectively stains mitochondria independent of their membrane potential and gives an index of mitochondrial mass based on staining intensity. After application, mitochondria can be imaged in live cells, or cells can be fixed and permeabilized for further study. This dye is suitable for long-term mitochondrial imaging and multiplex analysis with GFP expressed cells or other green-fluorescent probes. |

mitochondria. For example, MitoLite™ Green FM can be combined with the mitophagy-sensitive dye Mitophagy Red™ to monitor the mitochondria-lysosome interactions vital for maintaining homeostasis in eukaryotic cells. These include mitochondria-lysosome fusion, a process that selectively removes redundant or damaged mitochondria (Figure 3), or mitochondria-lysosome contact (MLC). MitoLite™ dyes can be combined with potential-dependent probes such as TMRE or TMRM to monitor mitochondrial structural integrity while also assessing mitochondrial membrane potential, as well as with the mitochondrial calcium indicator Rhod-2 am or with mitochondrial ROS sensors.

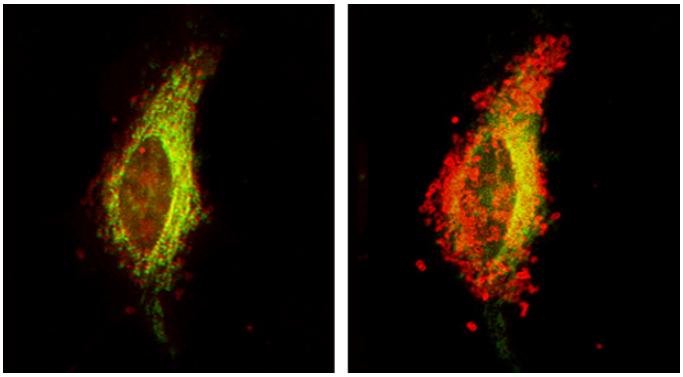

**Figure 3. Mitochondrial morphology during mitophagy.** HeLa cells labeled with MitoLite™ Green FM (green) and autophagy sensor Mitophagy Red™ (red) were treated with CCCP to depolarize mitochondria. Loss of mitochondrial membrane potential triggers the targeted clearance of damaged mitochondria via mitophagy, as reflected through the colocalization of both dyes.

**Table 2.** AAT Bioquest tools for studying mitochondrial function.

| Target | Tool | Ex/Em (mn) | Cat No. | Mechanism of action |
|---|---|---|---|---|
| Mitochondrial membrane potential | TMRM | 552/574 | 22221 | TMRM and TMRE are membrane-permeant, cationic rhodamine dyes for live-cell dynamic studies of mitochondrial membrane potential. They selectively accumulate in active mitochondria with intact membrane potential and, upon loss of potential, leaks into the cytoplasm. TMRM and TMRE are multiplexable with dyes that emit violet, blue, green, and deep red fluorescence, such as nucleic acid stains Hoechst 33342 and DAPI, the lipid stain Nile Green™, and lysosomal stain LysoBrite™ Deep Red. |
| | TMRE | 552/574 | 22220 | |
| | JC-1 | 515/530 | 22200 | JC-1 is a membrane-permeant, cationic carbocyanine dye for live-cell dynamic studies of mitochondrial membrane potential. It exhibits potential-dependent accumulation in mitochondria as indicated by a shift in fluorescence emission from 525 nm to 590 nm. At low concentrations due to low mitochondrial membrane potential, JC-1 exists as a monomer that yields green fluorescence with an emission of 530 nm. At high concentrations due to high mitochondrial membrane potential, JC-1 forms dye aggregates that yield orange fluorescence with an emission of 590 nm. |
| | JC™-10 | 508/524 | 22204 | JC-10™ is an improved version of JC-1 offering better water solubility. JC-10 exhibits the same potential-dependent accumulation in mitochondria and shift in fluorescence emission from 524 nm to 590 nm. It can be used to study live-cell dynamics of mitochondrial membrane potential in flow cytometry, fluorescence imaging, and microplate assays. |
| Mitochondrial calcium flux | Rhod-2 AM | 553/577 | 21060 | Rhod-2 AM is a membrane-permeant calcium indicator that has utility in measuring mitochondrial calcium flux because of its preferential accumulation in mitochondria. Because of the low solubility of AM esters, a mild surfactant such as Pluronic® F-127 is typically used to disperse the dye and facilitate cell loading. |
| Oxidative phosphorylation | MitoROS™ 520 | 488/530 | 16060 | Mitochondria generate various reactive oxygen species (ROS), particularly superoxides. MitoROS™ 520 is a membrane-permeant superoxide sensor for measuring mitochondrial superoxide levels in live cells. Upon reacting with superoxide, MitoROS™ 520 emits bright green fluorescence at 537 nm. |
| | MitoROS™ 580 | 500/582 | 16052 | MitoROS™ 580 is a red superoxide indicator that permeates live cells and selectively targets mitochondria. The rapid oxidation of MitoROS™ 580 by superoxides produces highly fluorescent products that emit bright red fluorescence at ~580 nm. |
| | MitoROS™ OH580 | 576/598 | 16055 | MitoROS™ OH580 is a membrane-permeant hydroxyl radical sensor that selectively targets mitochondria in live cells. Upon reacting with hydroxyl radicals, MitoROS™ OH580 emits bright red fluorescence at 598 nm. |
| Mitophagy (mitochondrial autophagy) | Mitophagy Red™ | 540/590 | 22998 | Mitophagy Red™ readily permeates live cells where it selectively targets mitochondria. During the induction of mitochondrial autophagy, Mitophagy Red™ translocates to lysosomal compartments, and when excited, emits bright red fluorescence at ~590 nm. This dye is suitable for multiplex analysis with green-fluorescent mitochondrial morphology probes, GFP expressed cells, or other green-fluorescent probes (Figure 3). |

## References


1. Bowser, D. N., Minamikawa, T., Nagley, P., & Williams, D. A. (1998). Role of mitochondria in calcium regulation of spontaneously contracting cardiac muscle cells. Biophysical journal, 75(4), 2004–2014. https://doi.org/10.1016/S0006-3495(98)77642-8
2. Glancy B. (2020). Visualizing Mitochondrial Form and Function within the Cell. Trends in molecular medicine, 26(1), 58–70. https://doi.org/10.1016/j.molmed.2019.09.009
3. Herst, P. M., Rowe, M. R., Carson, G. M., & Berridge, M. V. (2017). Functional Mitochondria in Health and Disease. Frontiers in endocrinology, 8, 296. https://doi.org/10.3389/fendo.2017.00296
4. Leonard, A. P., Cameron, R. B., Speiser, J. L., Wolf, B. J., Peterson, Y. K., Schnellmann, R. G., Beeson, C. C., & Rohrer, B. (2015). Quantitative analysis of mitochondrial morphology and membrane potential in living cells using high-content imaging, machine learning, and morphological binning. Biochimica et biophysica acta, 1853(2), 348–360. https://doi.org/10.1016/j.bbamcr.2014.11.002
5. Osellame, L. D., Blacker, T. S., & Duchen, M. R. (2012). Cellular and molecular mechanisms of mitochondrial function. Best practice & research. Clinical endocrinology & metabolism, 26(6), 711–723. https://doi.org/10.1016/j.beem.2012.05.003
6. Picard, M., Shirihai, O. S., Gentil, B. J., & Burellet, Y. (2013). Mitochondrial morphology transitions and functions: implications for retrograde signaling?. American journal of physiology. Regulatory, integrative and comparative physiology, 304(6), R393–R406. https://doi.org/10.1152/ajpregu.00584.2012


| Product | Unit Size | Cat No. |
|---|---|---|
| MitoROS™ 580 *Optimized for Detecting Reactive Oxygen Species (ROS) in Mitochondria* | 500 Tests | 16052 |
| Cell Meter™ Mitochondrial Hydroxyl Radical Detection Kit *Red Fluorescence* | 200 Tests | 16055 |
| Cell Meter™ Fluorimetric Mitochondrial Superoxide Activity Assay Kit *Green Fluorescence* | 200 Tests | 16060 |
| Rhod-2, AM *CAS#: 145037-81-6* | 1 mg | 21060 |
| Rhod-2, AM *UltraPure Grade* *CAS#: 145037-81-6* | 1 mg | 21062 |
| Rhod-2, AM *UltraPure Grade* *CAS#: 145037-81-6* | 50 mg | 21063 |
| Rhod-2, AM *UltraPure Grade* *CAS#: 145037-81-6* | 20x50 ug | 21064 |
| JC-1 [5,5,6,6-Tetrachloro-1,1,3,3-tetraethylbenzimidazolylcarbocyanine iodide] *CAS#: 3520-43-2* | 5 mg | 22200 |
| JC-1 [5,5,6,6-Tetrachloro-1,1,3,3-tetraethylbenzimidazolylcarbocyanine iodide] *CAS#: 3520-43-2* | 50 mg | 22201 |
| JC-10 *Superior alternative to JC-1* | 5x100 uL | 22204 |
| TMRE [Tetramethylrhodamine ethyl ester] *CAS#: 115532-52-0* | 25 mg | 22220 |
| TMRM [Tetramethylrhodamine methyl ester] *CAS#: 115532-50-8* | 25 mg | 22221 |
| MitoLite™ Blue FX490 | 500 Tests | 22674 |
| MitoLite™ Green EX488 | 500 Tests | 22675 |
| MitoLite™ Orange FX570 | 500 Tests | 22676 |
| MitoLite™ Red FX600 | 500 Tests | 22677 |
| MitoLite™ Deep Red FX660 | 500 Tests | 22678 |
| MitoLite™ Orange EX405 | 500 Tests | 22679 |
| MitoLite™ NIR FX690 | 500 Tests | 22690 |
| MitoLite™ Green FM | 10x50 ug | 22695 |
| MitoLite™ Red CMXRos | 10x50 ug | 22698 |
| Cell Meter™ Mitochondrial Autophagy Imaging Kit *Red Fluorescence* | 100 Tests | 22998 |
| CytoFix™ Red Mitochondrial Stain | 500 Tests | 23200 |

## Previous Issue


### AssayWise 10(1)

### Featured Articles

**Low-cost, ultra-sensitive fluorescence detection of DNA by gel electrophoresis using environmentally benign Gelite™ Safe DNA Gel Stain**

**Enzymatic and Chemical Labeling Strategies for Oligonucleotides**

**Sensitive Identification of Newly Synthesized DNA In Situ using click chemistry-based Bucculite™ XdU Cell Proliferation Assays**

**A Practical Guide for the Detection and Analysis of PCR Products**

**AAT Bioqeust, Inc.**
520 Mercury Drive
Sunnyvale, CA 94085
United States
Tel: +1 800 990 8053
Fax: +1 800 609 2943
Email: support@aatbio.com

**For Research Use Only. Not for use in diagnostic or therapeutic procedures.**

# International Distributors

**Australia:**
Assay Matrix Pty Ltd.
Email: info@assaymatrix.com
Website: http://www.assaymatrix.com

Jomar Life Research
Email: info@liferesearch.com
Website: http://www.liferesearch.com

**Austria:**
Biomol GmbH
Email: info@biomol.de
Website: http://www.biomol.de

**Belgium:**
Gentaur BVBA
Email: info@gentaur.com
Website: http://www.gentaur.com

**Canada:**
Cedarlane Laboratories Ltd.
Email: sales@cedarlanelabs.com
Website: http://www.cedarlanelabs.com

**China:**
Tianjin Biolite Biotech Co., Ltd
Email: info@tjbiolite.com
Website: http://www.tjbiolite.com

**Croatia:**
Biomol GmbH
Email: info@biomol.de
Website: http://www.biomol.de

**Czech Republic:**
Scintila, s.r.o.
Email: rejtharkova@scintila.cz
Website: http://www.scintila.cz

**Denmark:**
Nordic BioSite ApS
Email: info@nordicbiosite.dk
Website: http://www.nordicbiosite.dk

**Estonia:**
Biomol GmbH
Email: info@biomol.de
Website: http://www.biomol.de

Nordic BioSite AB
Email: info@biosite.se
Website: http://www.biosite.se

**Finland:**
Nordic BioSite OY
Email: info@biosite.fi
Website: http://www.biosite.fi

**France:**
EUROMEDEX
Email: research@euromedex.com
Website: http://www.euromedex.com

Interchim
Email: interchim@interchim.com
Website: http://www.interchim.com

**Germany:**
Biomol GmbH
Email: info@biomol.de
Website: http://www.biomol.de

**Hong Kong:**
Mai Bio Co., Ltd
Email: info@maibio.com
Website: http://www.maibio.com

**Hungary:**
IZINTA Trading Co., Ltd.
Email: baloghk@izinta.hu
Website: http://www.izinta.hu

**Iceland:**
Nordic BioSite AB
Email: info@biosite.se
Website: http://www.biosite.se

**India:**
Biochem Life Sciences
Email: info@bcls.in
Website: http://www.bcls.in

GenxBio Health Sciences Pvt. Ltd,
Email: sales@genxbio.com
Email: genxbio@gmail.com
Website: http://www.genxbio.com

**Ireland:**
Stratech Scientific Ltd.
Email: info@stratech.co.uk
Website: http://www.stratech.co.uk

**Israel:**
ADVANSYS Technologies for Life Ltd.
Email: info@advansys.co.il
Website: http://www.advansys.co.il

**Italy:**
Space Import Export S.r.l.
Email: info@spacesrl.com
Website: http://www.spacesrl.com

Valter Occhiena S.r.l.
Email: vo@valterocchiena.com
Website: http://www.valterocchiena.com

**Japan:**
Cosmo Bio Co., Ltd.
Email: mail@cosmobio.co.jp
Website: http://www.cosmobio.co.jp

Nacalai Tesque, Inc.
Email: info@nacalaiusa.com
Website: http://www.nacalai.com

Wako Pure Chemical Industries, Ltd.
Email: labchem-tec@wako-chem.co.jp
Website: http://www.wako-chem.co.jp

**Korea:**
Cheong Myung Science Corporation
Email: cms@cmscorp.co.kr
Website: http://www.cmscorp.co.kr

Kimnfriends Corporation
Email: kimnfriends@hanmail.net
Website: http://www.kimnfriends.co.kr

**Latvia and Lithuania:**
Nordic BioSite AB
Email: info@biosite.se
Website: http://www.biosite.se

**Netherlands:**
ITK Diagnostics BV
Email: info@itk.nl
Website: http://www.itk.nl

**Norway:**
Nordic BioSite AB
Email: info@biosite.se
Website: http://www.biosite.se

**Poland and Slovenia:**
Biomol GmbH
Email: info@biomol.de
Website: http://www.biomol.de

**Romania:**
SC VitroBioChem SRL
Email: office@vitro.ro
Website: http://www.vitro.ro

**Singapore and Other South Asian Countries:**
Axil Scientific Pte Ltd.
Email: info@axilscientific.com
Website: http://www.axilscientific.com

**Slovakia:**
Scintila, s.r.o.
Email: rejtharkova@scintila.cz
Website: http://www.scintila.cz

**South American Countries and Regions:**
Impex Comércio Internacional Ltda.
Email: impexcom@terra.com.br
Website: http://www.impexbrasil.com.br

**Spain and Portugal:**
Deltaclon S. L
Email: info@deltaclon.com
Website: http://www.deltaclon.com

**Sweden:**
Nordic BioSite AB
Email: info@biosite.se
Website: http://www.biosite.se

**Switzerland:**
LuBioScience GmbH
Email: info@lubio.ch
Website: http://www.lubio.ch

**Taiwan:**
Cold Spring Biotech Corp.
Email: csbiotech@csbiotech.com.tw
Website: http://www.csbiotech.com.tw

Rainbow Biotechnology Co., LTD.
Email: rainbow@rainbowbiotech.com.tw
Website: http://www.rainbowbiotech.com.tw

**Turkey:**
Suarge Biyoteknoloji Ltd. Co.
Email: info@suarge.com
Website: http://www.suarge.com/en/

**United Kingdom:**
Stratech Scientific Ltd.
Email: info@stratech.co.uk
Website: http://www.stratech.co.uk